Kinetics Studies of the Cardiac Ca-ATPase Expressed in Sf21 Cells: New Insights on Ca-ATPase Regulation by Phospholamban

James E. Mahaney,* Joseph M. Autry,† and Larry R. Jones†

*Department of Biochemistry, West Virginia University School of Medicine, Morgantown, West Virginia 26506-9142, and †Department of Medicine and the Krannert Institute of Cardiology, Indiana University School of Medicine, Indianapolis, Indiana 46202 USA

ABSTRACT Kinetics studies of the cardiac Ca-ATPase expressed in Sf21 cells (*Spodoptera frugiperda* insect cells) have been carried out to test the hypotheses that phospholamban inhibits Ca-ATPase cycling by decreasing the rate of the E1·Ca to E1′·Ca transition and/or the rate of phosphoenzyme hydrolysis. Three sample types were studied: Ca-ATPase expressed alone, Ca-ATPase coexpressed with wild-type phospholamban (the natural pentameric inhibitor), and Ca-ATPase coexpressed with the L37A-phospholamban mutant (a more potent monomeric inhibitor, in which Leu^{37} is replaced by Ala). Phospholamban coupling to the Ca-ATPase was controlled using a monoclonal antibody against phospholamban. Gel electrophoresis and immunoblotting confirmed an equivalent ratio of Ca-ATPase and phospholamban in each sample (1 mol Ca-ATPase to 1.5 mol phospholamban). Steady-state ATPase activity assays at 37°C, using 5 mM MgATP, showed that the phospholamban-containing samples had nearly equivalent maximum activity (~0.75 μmol·nmol Ca-ATPase^{-1}·min^{-1} at 15 μM Ca^{2+}), but that wild-type phospholamban and L37A-phospholamban increased the Ca-ATPase K_{Ca} values by 200 nM and 400 nM, respectively. When steady-state Ca-ATPase phosphoenzyme levels were measured at 0°C, using 1 μM MgATP, the K_{Ca} values also shifted by 200 nM and 400 nM, respectively, similar to the results obtained by measuring ATP hydrolysis at 37°C. Measurements of the time course of phosphoenzyme formation at 0°C, using 1 μM MgATP and 268 nM ionized [Ca^{2+}], indicated that L37A-phospholamban decreased the steady-state phosphoenzyme level to a greater extent (45%) than did wild-type phospholamban (33%), but neither wild-type nor L37A-phospholamban had any effect on the apparent rate of phosphoenzyme formation relative to that of Ca-ATPase expressed alone. Measurements of inorganic phosphate (P_i) release concomitant with the phosphoenzyme formation studies showed that L37A-phospholamban decreased the steady-state rate of P_i release to a greater extent (45%) than did wild-type phospholamban (33%). However, independent measurements of Ca-ATPase dephosphorylation after the addition of 5 mM EGTA to the phosphorylated enzyme showed that neither wild-type phospholamban nor L37A-phospholamban had any effect on the rate of phosphoenzyme decay relative to Ca-ATPase expressed alone. Computer simulation of the kinetics data indicated that phospholamban and L37A-phospholamban decreased twofold and fourfold, respectively, the equilibrium binding of the first Ca^{2+} ion to the Ca-ATPase E1 intermediate, rather than inhibiting rate of the E·Ca to E′·Ca transition or the rate of phosphoenzyme decay. Therefore, we conclude that phospholamban inhibits Ca-ATPase cycling by decreasing Ca-ATPase Ca^{2+} binding to the E1 intermediate.

INTRODUCTION

Phospholamban is a 52-amino acid integral membrane protein of cardiac sarcoplasmic reticulum (SR), which is the principal regulator of the Ca-ATPase in this membrane system. The Ca-ATPase is a 110-kDa integral membrane protein of cardiac SR that transports Ca^{2+} ions into the SR to promote cardiac muscle relaxation (reviewed by Simmerman and Jones, 1998). Phospholamban interacts with the Ca-ATPase at specific cytoplasmic binding sites (Toyofuku et al., 1994a,b), but transmembrane interactions between the two proteins also appear to be intimately involved in the inhibition process (Kimura et al., 1996). It has been well demonstrated that dephosphorylated phospholamban inhibits Ca-ATPase activity by decreasing enzyme sensitivity to Ca^{2+} for activation of ATP hydrolysis (MacLennan et al., 1992; Voss et al., 1994; Autry and Jones, 1997). The inhibition of the Ca-ATPase is relieved by phosphorylation of phospholamban at Ser^{16} or Thr^{17} or by the binding of a monoclonal antibody against the cytoplasmic domain of phospholamban (Autry and Jones, 1997), resulting in a marked increase in Ca-ATPase activity. The majority of studies have shown that phospholamban does not alter Ca-ATPase V_{max} significantly; it alters only the [Ca^{2+}] required to produce maximum activity (Kranias, 1985; MacLennan et al., 1992; Jones and Field, 1993; Cantilina et al., 1993; Reddy et al., 1996; Autry and Jones, 1997; Chu et al., 1998), although this point is still contested (Antipenko et al., 1997a; Simmerman and Jones, 1998).

Despite our knowledge of the functional effects of phospholamban on Ca-ATPase activity, fundamental questions remain about the mechanism by which phospholamban exerts its inhibitory interaction (Scheme 1). A number of investigators have previously studied the effect of phospholamban on the partial reactions of the Ca-ATPase cycle (Shigekawa et al., 1976; Jones et al., 1978; Sumida et al., 1978, 1980; Tada et al., 1979, 1980; Kranias et al., 1980; Cantilina et al., 1993; Hughes et al., 1994; Antipenko et al., 1997a, 1999). Unfortunately, these studies have provided

Received for publication 30 August 1999 and in final form 1 December 1999.

Address reprint requests to Dr. James E. Mahaney, Department of Biochemistry, West Virginia University School of Medicine, P.O. Box 9142, Morgantown, WV 26506-9142. Tel.: 304-293-7756; Fax: 304-293-6846; E-mail: jmahaney@hsc.wvu.edu.

0006-3495/00/03/1306/18 $2.00

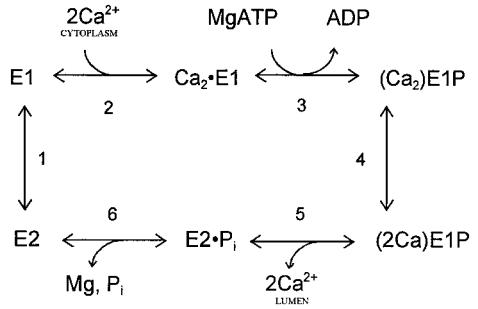

Scheme 1.

conflicting results about which Ca-ATPase partial reaction(s) are affected by phospholamban, and thus a unified model has been slow to emerge. Several studies (Tada et al., 1979; Antipenko et al., 1997a, 1999) have suggested that phospholamban controls Ca-ATPase activity by decreasing by twofold the rate of phosphoenzyme decomposition. Kinetics studies of Ca-ATPase in skeletal muscle SR by Froehlich and Taylor (1975, 1976) have shown that Ca-ATPase phosphoenzyme decomposition is a two-step process (steps 5 and 6, Scheme 1), in which E2P is first hydrolyzed to E2·P_i, followed by the release of inorganic phosphate (P_i) from the enzyme forming the E2 intermediate. The relative rates of these two steps are modulated by a variety of factors, including ionized [Ca^{2+}], suggesting that the inhibition of Ca-ATPase phosphoenzyme decomposition by phospholamban can account for the effect of phospholamban on the [Ca^{2+}] dependence of Ca-ATPase activity (Simmerman and Jones, 1998). In contrast, however, a number of investigators (Cantilina et al., 1993; Negash et al., 1996; Antipenko et al., 1997a) have provided evidence that phospholamban inhibits Ca-ATPase cycling by increasing the activation energy of a slow Ca^{2+}-dependent conformational change, which is required for ATP-dependent phosphoenzyme formation, and which occurs during the E1 + $2Ca^{2+}$ to E1·Ca_2 transition (step 2, Scheme 1). Previously, Inesi et al. (1980) showed that the cooperative binding of two Ca^{2+} ions to the Ca-ATPase occurs in two discrete steps separated by a conformational change (Scheme 2). The binding of the first Ca^{2+} ion to the Ca-ATPase E1 intermediate (forming E1·Ca) stimulates a conformational change in the enzyme (E1·Ca to E1′·Ca), which increases the affinity of the enzyme for binding the second Ca^{2+} ion, forming E1′·Ca_2. Subsequently, Cantilina et al. (1993) proposed that phospholamban decreases by 10-fold the forward and reverse rate constants for the E1·Ca to E1′·Ca transition. While this model can account for the shift in the [Ca^{2+}] dependence of Ca-ATPase activity induced by phospholamban, the proposal remains to be tested quantitatively. Clearly, these mechanistic issues have to be resolved to provide a better understanding of the inhibition of Ca-ATPase by phospholamban.

$$E1 + Ca^{2+} \rightleftharpoons E1{\cdot}Ca$$

$$E1{\cdot}Ca \rightleftharpoons E1'{\cdot}Ca$$

$$E1'{\cdot}Ca + Ca^{2+} \rightleftharpoons E1'{\cdot}Ca_2$$

Scheme 2.

In the present work, we have carried out kinetics studies of the cardiac Ca-ATPase to test the hypotheses that phospholamban inhibits Ca-ATPase cycling by decreasing the rate of the E1·Ca to E1′·Ca transition and/or the rate of phosphoenzyme hydrolysis. To assist in these studies, we have made use of the baculovirus-Sf21 insect cell (*Spodoptera frugiperda* insect cell) expression system to study Ca-ATPase-phospholamban functional interactions. An advantage of this system is that sufficient expressed material is produced to allow detailed kinetics characterizations, including phosphoenzyme formation and decomposition studies. Expression systems previously used to study the regulatory effects of phospholamban on the Ca-ATPase have yielded much lower levels of protein (discussed in Autry and Jones, 1997), precluding the type of kinetics studies presently reported. In addition, this expression system facilitates the study of the phosphorylation and dephosphorylation kinetics of the cardiac Ca-ATPase expressed by itself, independently of the influence of phospholamban, compared directly with parallel kinetics studies of the Ca-ATPase coexpressed with wild-type pentameric phospholamban (the natural inhibitor) or with the monomeric L37A-phospholamban mutant (a potent superactive mutant or "super shifter") (Simmerman et al., 1996; Autry and Jones, 1997; Kimura et al., 1997). Any effect of wild-type phospholamban on Ca-ATPase kinetics would be expected to be amplified in the presence of the more potent L37A-phospholamban and absent when the Ca-ATPase is expressed alone without phospholamban. Finally, to further document the specific effect of phospholamban on Ca-ATPase kinetics, we took advantage of our monoclonal antibody 2D12 raised against phospholamban (Sham et al., 1991; Briggs et al., 1992), which selectively reverses phospholamban inhibitory effects on Ca-ATPase, like phospholamban phosphorylation (Cantilina et al., 1993; Antipenko et al., 1997b). Use of the anti-phospholamban antibody allowed large amounts of membrane material to be utilized for kinetics studies, removing the need for protein kinase activation and inhibition of phosphatase activity during lengthy kinetics experiments. Our results show that phospholamban acts by decreasing Ca-ATPase affinity for Ca^{2+}, not by slowing the rate of the E1·Ca to E1′·Ca conformational transition (Cantilina et al., 1993; Negash et al., 1996; Antipenko et al., 1997a) or the rate of dephosphorylation of the E2P intermediate (Tada et al., 1979; Antipenko et al., 1997a, 1999), as previously proposed by others.

MATERIALS AND METHODS

Materials

[γ-^{32}P]ATP was purchased from ICN, and ^{125}I-labeled protein A was purchased from DuPont NEN. Prestained molecular weight standards and polyvinylidene difluoride (PVDF) membranes were purchased from Bio-Rad. Sf21 insect cells were purchased from Invitrogen, and the BaculoGold system was obtained from Pharmigen.

Protein expression and isolation

Recombinant baculoviruses containing cDNA inserts for canine cardiac Ca-ATPase (SERCA2a) or canine phospholamban were prepared using the BaculoGold system as recently described (Autry and Jones, 1997). Wild-type canine SERCA2a and canine phospholamban (wild type and mutant) were expressed in Sf21 cells grown in suspension (1.5×10^6 cells/ml) at 27°C in Grace's insect cell medium (Life Technologies) supplemented with 10% fetal bovine serum (Atlanta Biologicals) and containing 0.1% Pluronic F-68 (Life Technologies). Microsomes were isolated from insect cells harvested 48 h after infection with baculoviruses. For expression of the Ca-ATPase alone, a multiplicity of infection of 10 (viruses per cell) was used. For coexpression of the Ca-ATPase and phospholamban, a multiplicity of infection of 15 was used for SERCA2a and 5 for phospholamban (wild type and mutant). Virus-infected Sf21 cells in 600 ml of suspension (9×10^8 cells) were sedimented and then washed twice with an ice-cold solution containing 137 mM NaCl, 2.7 mM KCl, 4.3 mM Na_2HPO_4, 1.4 mM KH_2PO_4 (pH 7.4), by centrifugation for 5 min at 1500 rpm at 4°C in an IEC GP8R refrigerated centrifuge. The washed cells were resuspended in 100 ml of ice-cold 10 mM $NaHCO_3$ containing 10 μg/ml aprotinin, 2 μg/ml leupeptin, 1 μg/ml pepstatin A, and 0.1 mM pefabloc, and then homogenized for 90 s with a Brinkman Polytron (~50% full speed) in a cold room. The homogenate was centrifuged for 20 min at 9000 rpm ($10{,}000 \times g$), 4°C, in a Sorvall SS34 rotor. The supernatant was collected and the Sf21 insect cell microsomes were pelleted by centrifugation for 35 min at 26,000 rpm ($70{,}000 \times g$), 4°C, in a Beckman Ti45 rotor. The pellets were resuspended to ~5 mg/ml in 250 mM sucrose, 30 mM histidine (pH 7.4) and stored in small aliquots at −50°C. Protein concentrations were determined by the method of Lowry et al. (1951), using bovine serum albumin (Sigma) as a standard. The average yield per 600 ml of infection was 30 mg of microsomal protein. Additional details of the purification and characterization of Sf21 insect cell microsomes are provided elsewhere (Autry and Jones, 1997).

Electrophoresis and immunoblotting

Before electrophoresis, samples were solubilized at 37°C for 5 min in a dissociation medium that contained 62.5 mM Tris (pH 6.8), 5% glycerol, 5% sodium dodecyl sulfate (SDS), 40 mM dithiothreitol, and 0.0025% bromphenol blue. Sodium dodecyl sulfate-polyacrylamide gel electrophoresis (SDS-PAGE) (BioRad Mini-Protean II System) was conducted by the method of Porzio and Pearson (1977), using 8% polyacrylamide. Kaleidoscope prestained molecular weight markers (BioRad) were used as standards. Gels were stained using GelCode Blue Stain reagent (Pierce), or proteins were transferred (BioRad Mini-Transblot System) to PVDF membranes (BioRad) for immunoblotting. The transfer protocol was carried out according to the instructions provided by the manufacturer, except that methanol was excluded from the transfer buffer. We found that the use of methanol in the transfer buffer resulted in a significant amount of protein being retained in the polyacrylamide gel after transfer. In addition, a second membrane sheet was used for each blot, to capture protein that migrated through the first sheet without binding. The PVDF membranes were probed with anti-SERCA2a monoclonal antibody 2A7-A1 for detection of SERCA2a or with anti-phospholamban monoclonal antibody 2D12 for detection of phospholamban (Movsesian et al., 1994). Antibody-binding proteins were visualized using [^{125}I]-protein A, and labeling intensities from both membranes were quantified and summed using a Molecular Dynamics Phosphorimager SI. For quantitative immunoblotting, SERCA2a was purified from canine cardiac SR vesicles, and recombinant canine phospholamban was purified from Sf21 insect cells by 2A7-A1 or 2D12 monoclonal antibody affinity chromatography, respectively. These samples were used as standards to quantify the amount of SERCA2a and phospholamban in the Sf21 insect cell microsomes (described below). We found that for SERCA2a, 80% of the blot intensity appeared on the first membrane, and the remaining 20% on the second membrane. For pentameric phospholamban, more than 99% of the blot intensity appeared on the first membrane, with only a faint trace of blot intensity on the second membrane. For monomeric phospholamban, 85% of the blot intensity appeared on the first membrane, with the remaining 15% of the intensity localized to the second membrane. No GelCode Blue-stained protein bands in the vicinity of SERCA2a or phospholamban were retained on the polyacrylamide gel after transfer to the PVDF membranes.

SERCA2a ATPase assay

[Ca^{2+}]-dependent ATPase activity of SERCA2a in the Sf21 insect cell microsomes was measured colorimetrically at 37°C, using a malachite green-ammonium molybdate assay (Lanzetta et al., 1979; Mahaney et al., 1995). SERCA2a incubation tubes contained 0.05 mg/ml protein in 50 mM 3-[*N*-morpholino]propanesulfonic acid (MOPS) (pH 7.0), 3 mM $MgCl_2$, 100 mM KCl, 1 mM EGTA, and 0–1.0 mM $CaCl_2$, to give the desired ionized [Ca^{2+}], as previously determined (Autry and Jones, 1997). To initiate the ATPase reaction, 5 mM MgATP was added to the incubation tube. After 10 min of reaction at 37°C, a 50-μl aliquot of the incubation mixture was transferred into an assay tube containing 1.6 ml of malachite green-ammonium molybdate reagent at room temperature. After 30 s, the colorimetric reaction was quenched by the addition of 200 μl of 34% sodium citrate (Sigma) into the assay tube. For the determination of phosphate, a standard curve was constructed using aliquots of a 0.65 mM phosphate standard solution (Sigma), assayed in a similar fashion. After 30 min of color development, the absorbance of the malachite green reagent was measured at 660 nm. SERCA2a samples were pretreated with the Ca^{2+} ionophore A23187 (CalBiochem) (20 μg/mg of total protein) before addition to the incubation tubes. Before preparation of the incubation tubes, the SERCA2a samples were incubated for 20 min on ice without or with affinity-purified anti-phospholamban monoclonal antibody 2D12, at an antibody-to-total protein weight ratio of 1:1 (Autry and Jones, 1997).

ATP-dependent phosphoenzyme formation

Ca-ATPase phosphoenzyme formation experiments were carried out using ice-cold solutions. Mixing was conducted in a cold room (2 ± 1°C) to prevent significant sample warming during additions and vortexing. Before phosphoenzyme formation, the SERCA2a-containing Sf21 insect cell microsomes were permeabilized by the addition of Ca^{2+} ionophore A23187 (20 μg/mg total protein). Next, 0.25 ml of a solution containing 0.2 mg Sf21 microsomes/ml in 50 mM MOPS (pH 7.0), 3 mM $MgCl_2$, 100 mM KCl, 1 mM EGTA was placed in a 7-ml glass scintillation vial (VWR) and set on ice. The EGTA preincubation was designed to remove all traces of Ca^{2+} from the medium and to stabilize SERCA2a in a Ca^{2+}-free state. To initiate phosphoenzyme formation, 0.25 ml of an ice-cold solution containing 50 mM MOPS (pH 7.25), 3 mM $MgCl_2$, 100 mM KCl, 1 mM EGTA, varying $CaCl_2$, and 2 μM [γ-^{32}P]ATP (20,000 cpm/nmol) was added rapidly (less than 1 s) to the microsome-containing vial with intermittent vortexing. The final conditions after mixing were 50 mM MOPS (pH 7.0), 3 mM $MgCl_2$, 100 mM KCl, 1 mM EGTA, and either 0.5 mM $CaCl_2$ (ionized $[Ca^{2+}]_{final} = 268$ nM), 0.7 mM $CaCl_2$ (ionized $[Ca^{2+}]_{final} = 625$ nM), or 1 mM $CaCl_2$ (ionized $[Ca^{2+}]_{final} = 15$ μM). The reaction

was allowed to proceed for different times before quenching by the rapid addition of 0.5 ml of ice-cold 9% perchloric acid + 6 mM H_3PO_4, followed by vigorous vortexing. Blank tubes were prepared by first adding 0.5 ml of quench solution to the 0.25-ml microsome-containing solution, vortexing vigorously, then adding 0.25 ml of the ATP-containing solution. A 25-μl aliquot of 10 mg/ml bovine serum albumin was added to each quenched sample to act as a carrier protein during the processing of the sample vials. The quenched samples were pelleted by centrifugation for 10 min at 3000 $\times$ *g*, 4°C, in an IEC GP8R refrigerated centrifuge, and then washed three times by similar centrifugation using an ice-cold solution of 5% trichloroacetic acid, 6% polyphosphoric acid, 4 mM H_3PO_4, and 5 mM nonradioactive ATP. Pellet recovery after washing was greater than 95%, determined by protein assay. The final pellets were dissolved in 5 ml 1 N NaOH, and the [^{32}P]phosphoenzyme was assayed by counting the Cerenkov radiation.

Separation and analysis of $^{32}P_i$ in the presence of [γ-^{32}P]ATP

[^{32}P]P_i liberation during phosphoenzyme formation was assayed according to Mahaney et al. (1995). After the first sedimentation of the quenched phosphorylation sample, 0.5 ml of the supernatant was added to 0.5 ml of a 2% aqueous charcoal slurry. The sample was vortexed and centrifuged for 10 min at 3000 $\times$ *g*, 4°C. A 0.5-ml aliquot of the supernatant was added to another 0.5 ml of a 2% aqueous charcoal slurry, vortexed, and centrifuged as before. A 0.5-ml aliquot of the supernatant from this second centrifugation was added to 0.75 ml of water saturated with 1:1 isobutanol: xylene contained in a 16 $\times$ 100 mm borosilicate assay tube and vortexed. To each tube was added 0.4 ml of 5% ammonium molybdate (in 4 N HCl) reagent, and the samples were vortexed briefly. Complex formation between P_i and the molybdate (yellow color development) was allowed to proceed for 15 min. After the incubation, 2 ml of water-saturated 1:1 isobutane:xylene was added to each tube and vortexed 3 $\times$ 10 s with 10 s between vortexing periods. The phases were allowed to separate for 10 min, after which 1 ml of the organic (upper) phase was pipetted into 5 ml of 1 N NaOH contained in a 7-ml glass scintillation vial. The vials were capped and shaken until the yellow color disappeared, and ^{32}P was assayed by counting the Cerenkov radiation. All steps involving organic solvents were carried out in a fume hood, and tubes containing solvents were covered when not in use, to minimize solvent loss due to evaporation.

Dephosphorylation of the phosphoenzyme by EGTA

SERCA2a samples were phosphorylated with 1 μM [γ-^{32}P]ATP at 0°C for 30 s as described above, followed by the rapid addition of 0.25 ml of solution containing 50 mM MOPS (pH 7.0), 3 mM $MgCl_2$, 100 mM KCl, variable $CaCl_2$ (as defined above), and 15 mM EGTA. The final [EGTA] after mixing was 5 mM, which was sufficient to reduce the ionized [Ca^{2+}] to less than 1 nM. The reaction was allowed to proceed for various time periods before quenching by the rapid addition of 0.75 ml of ice-cold 9% perchloric acid + 6 mM H_3PO_4, followed by vigorous vortexing. A zero-time sample was obtained by quenching the phosphorylation reaction at 30 s and adding 0.5 ml of the EGTA chase solution to the quenched sample. Sample blanks were prepared as described above, except for the addition of 0.5 ml of the EGTA-containing solution to the quenched sample. The quenched samples were processed and assayed for ^{32}P-containing enzyme as described above.

Curve fitting and kinetic modeling

[Ca^{2+}]-dependent ATPase activity data and phosphoenzyme kinetics data were fit using the program KFIT written by N. C. Millar. The amplitude and rate parameters were constrained to positive numbers and allowed to vary without bound during the fits. The best fits of the data were chosen on the basis of optimization of the determination coefficient, R^2, and/or minimization of the sum-of-squares error, χ^2. Simulation of the time courses of phosphoenzyme formation, P_i liberation, and EP decay were carried out using the program KINSIM (Barshop et al., 1983), the reactions of Scheme 3, and the rate constants presented in Table 6 (Results). Because the rate of the E1P-to-E2P transition (Scheme 1, step 4) is significantly faster (>300 s^{-1}; Mahaney et al., 1995) than any of the other steps under the conditions of our experiments (described below), the phosphorylated Ca-ATPase was treated as a single species in the simulations. Initial values for the rate constants were obtained in the present study (see Results) and from Cantilina et al. (1993). The rate constants reported by Cantilina et al. define the Ca-ATPase cycle at 25°C; thus these constants were reduced by a factor of 5 for the present simulations (0°C), based on the general assumption that the reaction rates decreased by a factor of 2 for each 10°C decrease in temperature (i.e., Q_{10} of 2). The EGTA + Ca^{2+} equilibration, which occurred upon the simultaneous addition of Ca^{2+} and ATP to the microsomes preequilibrated in EGTA, was not modeled in the simulations, because this equilibration is rapid (Smith et al., 1984; Harrison and Bers, 1989) relative to the reaction steps of the SERCA2a cycle under our experimental conditions. The amplitude and rate parameters were constrained to positive numbers and allowed to vary without bound during the simulations. The goodness of fit of the simulation to the data was judged by maximizing the R^2 value for the simulation.

RESULTS

Protein expression, characterization, and assay

For this study, SERCA2a was expressed in Sf21 insect cells alone, coexpressed with wild-type phospholamban, or coexpressed with monomeric mutant L37A-phospholamban (Autry and Jones, 1997), and isolated as Sf21 insect cell microsomes. SDS-PAGE (Fig. 1 *A*) and immunoblotting (Fig. 1 *B*) of the Sf21 microsomes indicated that Sf21 cells produced similar amounts of recombinant Ca-ATPase and phospholamban in the expressed samples. Furthermore, the gel and the blots of the microsomal samples (Fig. 1, *A* and *B, lanes 1–3*) confirmed that there was almost no high-molecular-weight SERCA2a aggregate in the expressed samples. The amount of SERCA2a and phospholamban in the Sf21 microsome samples was determined by quantitative immunoblotting (Fig. 1, *B–D*), using purified SERCA2a and phospholamban samples as standards. As shown in Fig. 1, the purified proteins (*empty symbols*) provided linear standard curves that showed SERCA2a microsomes contained 8.3% SERCA2a and no phospholamban, SERCA2a + wild-type phospholamban microsomes contained 3% SERCA2a and 0.26% phospholamban, and SERCA2a + L37A-phospholamban microsomes contained 4.6% SERCA2a and 0.36% phospholamban (Table 1). The blot data for the expressed samples shown in Fig. 1 (*C* and *D*) was obtained using 10 μg of microsomal protein. Similar experiments conducted using 5 μg of microsomal protein (not shown) provided nearly identical results. Thus, even though the SERCA2a blot intensity of the SERCA2a alone sample is greater than that of the standards used (Fig. 1 *C, diamonds*), the extrapolated slope of the standard curve

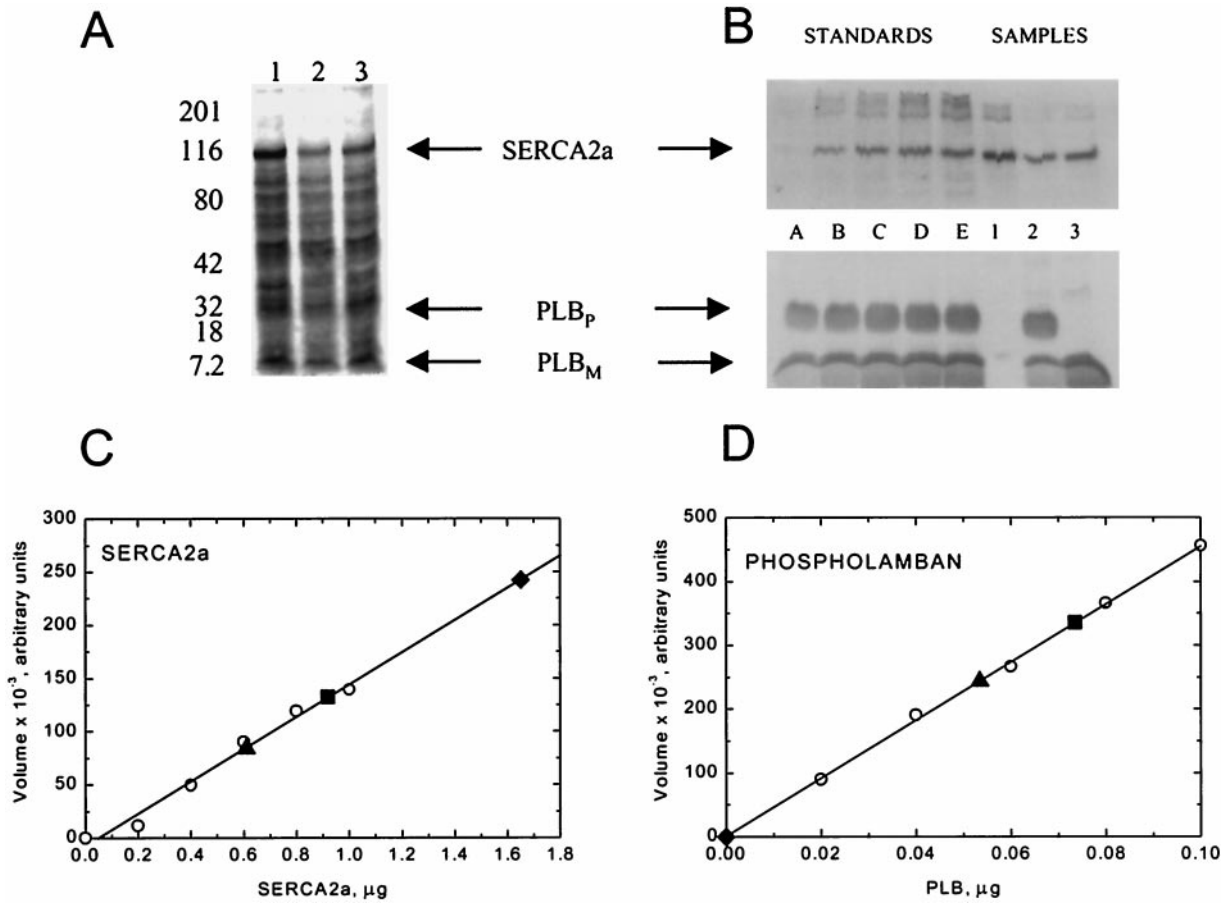

FIGURE 1 SDS-PAGE and immunoblotting of canine SERCA2a and phospholamban expressed in Sf21 microsomes. (*A*) GelCode Blue-stained SDS gel (10 μg protein per lane) showing Sf21 microsomes containing SERCA2a alone (*lane 1*), SERCA2a + wild-type phospholamban (*lane 2*), and SERCA2a + L37A-phospholamban (*lane 3*). (*B*) Corresponding immunoblot of the SDS gel shown in *A*, developed with SERCA2a antibody 2A7-A1 (*top*) or phospholamban antibody 2D12 (*bottom*). PLB_p denotes pentameric phospholamban and PLB_m denotes monomeric phospholamban. *Lanes A–E* contain 0.2–1.0 μg purified SERCA2a (*top*) or 0.02–0.1 μg purified phospholamban (*bottom*). *Lanes 1–3* contain 10 μg of Sf21 microsomal protein per lane and correspond to SERCA2a alone, SERCA2a + wild type phospholamban, and SERCA2a + L37A-phospholamban, respectively. (*C* and *D*) Standard curves (*empty symbols*) constructed using purified SERCA2a and phospholamban, respectively, showing the relationship between blot intensity and amount of protein loaded. The filled symbols correspond to the blot intensities obtained using Sf21 microsomes containing SERCA2a alone (♦), SERCA2a + wild type phospholamban (▲), and SERCA2a + L37A-phospholamban (■), which were used in conjunction with the standard curves to deduce the amount of SERCA2a or phospholamban in each of the sample types studied (Table 1). An identical experiment conducted using 5 μg of Sf21 microsomal protein per lane (not shown) produced equivalent results.

provides a reliable value for the amount of SERCA2a in this expressed sample. Using the molecular masses for canine SERCA2a (110,000 Da) (Autry and Jones, 1997) and phospholamban (6080 Da) (Fujii et al., 1987), we determined that the molar ratio of SERCA2a:phospholamban was 1:1.6 for the SERCA2a + wild-type phospholamban sample and 1:1.5 for the L37A-phospholamban sample. The similarity of the SERCA2a-to-phospholamban ratio in the two phospholamban-containing samples facilitated direct and quantitative comparison of the effects of wild-type versus L37A-phospholamban on SERCA2a phosphorylation kinetics.

To test the activity of the expressed SERCA2a and the functional coupling between SERCA2a and phospholamban in Sf21 cell microsomes, ATPase assays were conducted at 37°C at a series of [Ca^{2+}] in the presence and absence of anti-phospholamban monoclonal antibody 2D12, which reverses the inhibitory interaction between phospholamban and SERCA2a (Briggs et al., 1992; Sham et al., 1991). The ATPase activity of the expressed SERCA2a displayed the usual sigmoidal [Ca^{2+}] dependence, and the maximum steady-state activities per mg of microsomal protein for the three sample types were SERCA2a alone, 0.6 μmol·mg^{-1}·min^{-1}; SERCA2a + wild-type phospholamban, 0.2 μmol·mg^{-1}·min^{-1}; and SERCA2a + L37A-phospholamban, 0.3 μmol·mg^{-1}·min^{-1}. Differences in the maximum activities correlated with differences in Ca-ATPase expression levels between the different samples deduced from the SDS-PAGE and immunoblot analysis. That is, when corrected for the amount of SERCA2a in each sample type, the maximum activity for each sample was ~0.75

TABLE 1 Characterization of SERCA2a and phospholamban coexpressed in Sf21 insect cells

	Expression			SERCA2a ATPase Activity at 37°C and 5 mM MgATP			
Sample Type	SERCA2a (% total protein)	PLB (% total protein)	SERCA2a:PLB ratio (mol:mol)	V_{max} −Ab (μmol · nmol SERCA2a^{-1} · min^{-1})	V_{max} +Ab (μmol · nmol SERCA2a^{-1} · min^{-1})	K_{ca} −Ab (μM)	K_{ca} +Ab (μM)
SERCA2a alone	8.3	0.00	1:0	0.80 ± 0.05	0.80 ± 0.05	0.20 ± 0.02	0.19 ± 0.02
SERCA2a + WT-PLB	3.0	0.26	1:1.6	0.74 ± 0.10	0.74 ± 0.10	0.42 ± 0.03	0.22 ± 0.02
SERCA2a + L37A-PLB	4.6	0.36	1:1.5	0.72 ± 0.10	0.72 ± 0.10	0.80 ± 0.03	0.40 ± 0.03

Wild-type Ca-ATPase and phospholamban (wild-type or L37A-PLB) were coexpressed using the baculovirus-Sf21 insect cell expression system and isolated as insect cell microsomes. Sf21 insect cell microsomes were subjected to SDS-PAGE, and the protein bands were transferred from the gel onto PVDF membranes for immunoblotting. The amount of SERCA2a or phospholamban in the Sf21 microsomes was obtained from standard curves constructed using various amounts of purified SERCA2a (0–1 μg) or phospholamban (0–0.1 μg) included on the same gel as the expressed samples (Fig. 1). The molar ratio of SERCA2a to phospholamban in each sample was determined using the weight of each protein divided by the respective molecular weight (110,000 g/mol for SERCA2a (Autry and Jones, 1997) and 6080 g/mol for phospholamban (Fujii et al., 1987)). The SERCA2a ATPase activity of each sample was assayed at 37°C, using 5 mM MgATP and various $[Ca^{2+}]_{free}$ levels between 30 nM and 15 μM. Samples were preincubated in the absence (−Ab) or presence (+Ab) of anti-phospholamban monoclonal antibody, 2D12, for 20 min on ice before the start of the activity assays. The maximum activity (V_{max}) and $[Ca^{2+}]$ required for half-maximum activity (K_{Ca}) were determined from Hill fits of the $[Ca^{2+}]$-dependent ATPase activity for each sample. SERCA2a ATPase activity is expressed in terms of nmol SERCA2a, according to the amount of SERCA2a per mg of Sf21 cell microsomes for each sample. Errors denote the spread of triplicate determinations for a single experiment using a single preparation of expressed protein. Experimental repeats using different preparations gave very similar results.

μmol P_i produced per minute per nmol SERCA2a (Table 1). For comparison, a similar analysis was carried out using dog cardiac SR (CSR) vesicles. The ATPase activity of the CSR vesicles per mg of microsomal protein measured under identical conditions was 2.1 μmol·mg^{-1}·min^{-1}. When corrected for the amount of SERCA2a in this preparation of CSR, which was reported as 30% (Jones et al., 1979; Autry and Jones, 1997), the maximum activity of the sample was 0.77 μmol·nmol SERCA2a^{-1}·min^{-1}, which is identical to that of the expressed samples (Table 1). Thus there were no differences in SERCA2a specific activity between the expressed samples, which were identical to that in dog cardiac SR.

SERCA2a expressed without phospholamban had a high apparent Ca^{2+} affinity (ionized $[Ca^{2+}]$ giving half-maximum activation of the Ca-ATPase, K_{Ca} = 200 nM), which was unaffected by treatment of the sample with phospholamban monoclonal antibody (Table 1). When coexpressed with wild-type phospholamban, the SERCA2a activity curve was shifted to the right relative to that of SERCA2a expressed alone, resulting in an increase in K_{Ca} to 420 nM. When coexpressed with the monomeric mutant L37A-phospholamban, a potent super shifter (Autry and Jones, 1997; Kimura et al., 1997), the SERCA2a activity curve was shifted to the right to a greater extent, resulting in an increase in K_{Ca} to 800 nM. For both phospholamban-containing samples, treatment with anti-phospholamban antibody 2D12 shifted the Ca^{2+} activation curve to the left, resulting in twofold decreased K_{Ca} values. The K_{Ca} value for the antibody-treated SERCA2a + wild-type phospholamban sample was equivalent to that obtained for SERCA2a in the absence of phospholamban, whereas the K_{Ca} value for the antibody-treated SERCA2a + L37A-phospholamban sample was greater than that of the SERCA2a alone sample (Table 1). This characteristic of the SERCA2a + L37A-phospholamban sample has been reported previously (Autry and Jones, 1997), and it is a common feature of the super-shifting monomeric phospholamban mutants containing mutations in the leucine-isoleucine zipper domain (Autry and Jones, 1998). Note that the absolute amount of the K_{Ca} shift by the antibody for the L37A-phospholamban mutant (0.4 μM shift) was two times greater than the shift for wild-type phospholamban (0.2 μM shift). This demonstrates that the antibody effect on the L37A-phospholamban mutant is amplified compared to the antibody effect on wild-type phospholamban, even though the shift in Ca affinity by L37A-phospholamban on the Ca-ATPase is not reversed completely by the antibody. This suggests that the antibody is acting in a mechanistically realistic way on L37A-phospholamban/Ca-ATPase interactions, even though it is not capable of totally reversing the inhibitory effect of this potent mutant on Ca-ATPase activity. High ionized $[Ca^{2+}]$, however, is capable of reversing the inhibitory effect completely (see below). For comparison, the K_{Ca} values measured for dog cardiac SR were 400 nM and 170 nM for the sample without and with pretreatment with anti-phospholamban antibody, respectively, similar to the expressed SERCA2a + wild-type phospholamban sample. Ca-ATPase activities were identical between all three sets of microsomal membranes when measured at saturating ionized $[Ca^{2+}]$, and under this V_{max} condition the monoclonal antibody produced no effect (Table 1). Lack of effect of the monoclonal antibody on the Ca-ATPase V_{max} in native cardiac SR vesicles is well known (Simmerman and Jones, 1998). The results show that phospholamban was functionally coupled to Ca-ATPase in the two phospholamban-coexpressed samples, similar to that observed in native cardiac SR vesicles. Furthermore, the results confirm earlier

observations that the monomeric L37A-phospholamban mutant is a more potent inhibitor of steady-state Ca-ATPase activity than wild-type phospholamban, but even the more potent L37A-phospholamban does not affect the maximum ATPase activity (Autry and Jones, 1997; Kimura et al., 1997).

SERCA2a phosphoenzyme formation

The first goal of our kinetics studies was to test the hypothesis that phospholamban inhibits Ca-ATPase cycling by decreasing by 10-fold the rate of the E1·Ca-to-E1′·Ca transition (Cantilina et al., 1993). To test this hypothesis, we measured the effect of phospholamban on ATP-dependent SERCA2a phosphoenzyme (EP) formation, starting with the Ca-ATPase in a Ca^{2+}-free state. SERCA2a-containing microsomes were preincubated at 0°C in 1 mM EGTA in the experimental buffer to remove all traces of Ca^{2+} from the medium and to stabilize the Ca-ATPase in a Ca^{2+}-free state (Scheme 1). At time 0, an equal volume of the same ice-cold experimental buffer containing [γ-^{32}P]ATP (1 μM final) and Ca^{2+} (various levels) was added to the enzyme solution, and the reaction was allowed to proceed at 0°C for serial times before acid quenching and determination of phosphoenzyme formed. Samples were preincubated either without or with anti-phospholamban monoclonal antibody 2D12 before the initiation of phosphoenzyme formation. The low temperature and low [ATP] were used to slow the rate of EP formation and thus allow its measurement by hand mixing techniques over a 20–30-s time interval after the addition of ATP. The EGTA preincubation was included to allow us to measure the effect of phospholamban on the E1·Ca-to-E1′·Ca transition, which limits the rate of EP formation under these conditions (Cantilina et al., 1993; Tada et al., 1980). Specific control experiments of the expressed enzyme (not shown) showed that the EGTA preincubation had no deleterious effect on Ca-ATPase stability, even after a 1-h incubation on ice.

In the first set of experiments, we measured the effect of phospholamban on the [Ca^{2+}] dependence of steady-state EP levels formed by 1 μM ATP at 0°C for SERCA2a expressed in Sf21 cell microsomes (Fig. 2 and Table 2). The steady-state EP level of each sample type displayed a sigmoidal dependence on [Ca^{2+}], and the K_{Ca} values (Table 2) of the curves were nearly identical to those obtained from the [Ca^{2+}]-dependent ATPase activity of three SERCA2a samples measured at 37°C at saturating [ATP] (Table 1). The maximum steady-state EP level was similar for the three sample types, in terms of nmol EP formed per mg total Sf21 microsomal protein: 0.055 nmol EP/mg for SERCA2a alone, 0.02 nmol EP/mg for SERCA2a + wild type phospholamban, and 0.03 nmol EP/mg for SERCA2a + L37A-phospholamban. When the raw EP levels were corrected for Ca-ATPase expression levels in the different samples (Table 1), the three samples showed virtually identical maxi-

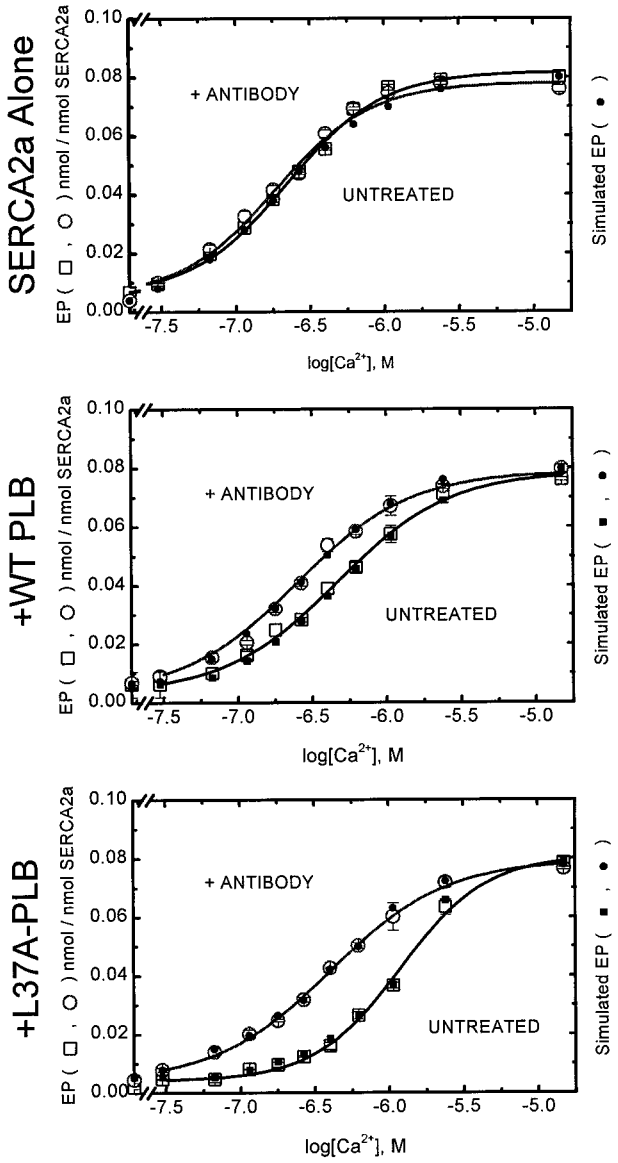

FIGURE 2 [Ca^{2+}] dependence of steady-state phosphoenzyme levels of SERCA2a in Sf21 microsomes formed by 1 μM ATP at 0°C. Steady-state SERCA2a phosphoenzyme (EP) levels were measured by phosphorylating Sf21 microsomes (0.1 mg/ml) preincubated in 1 mM EGTA with 1 μM [γ-^{32}P]ATP and various [Ca^{2+}] levels for 30 s at 0°C, followed by acid quenching and processing as described in Materials and Methods. (*A*) SERCA2a expressed alone; (*B*) SERCA2a coexpressed with wild-type phospholamban; (*C*) SERCA2a coexpressed with L37A-phospholamban. The steady-state EP levels of SERCA2a in Sf21 microsomes pretreated with phospholamban monoclonal antibody, 2D12, are denoted by empty circles (○), and the control, untreated microsomes are denoted by the empty squares (□). The data were simulated using the reactions of Scheme 3 and the rate constants in Table 6. Simulation of the antibody-treated data is denoted by the filled circles (●), and simulation of the control, untreated data is denoted by the filled squares (■). The curves represent fits of the data to the Hill equation, which provided the K_{Ca} and maximum EP values (Table 2). Empty symbols represent the average of triplicate measurements for a single preparation of each sample type. Error bars denote the high and low values in each average. Additional experiments using different preparations provided equivalent results.

TABLE 2 Inhibitory effects of phospholamban (wild-type or L37A-PLB) on the [Ca^{2+}] dependence of steady-state SERCA2a phosphoenzyme levels at 0°C using 1 μM Mg[γ-^{32}P]ATP

	Maximum EP level		K_{Ca}	
	−Ab	+Ab	−Ab	+Ab
	(nmol EP/nmol SERCA2a)		(μM)	
SERCA2a alone	0.075 ± 0.002	0.071 ± 0.002	0.22 ± 0.03	0.19 ± 0.03
SERCA2a + WT-PLB	0.076 ± 0.003	0.079 ± 0.003	0.46 ± 0.02	0.25 ± 0.02
SERCA2a + L37A-PLB	0.077 ± 0.003	0.075 ± 0.003	0.80 ± 0.03	0.40 ± 0.03

Sf21 insect cell microsomes containing SERCA2a alone or SERCA2a + phospholamban (wild-type or L37A-PLB) were phosphorylated for 30 s at 0°C, using 1 μM Mg[γ-^{32}P]ATP at various $[Ca^{2+}]_{free}$, as depicted in Fig. 2. The sigmoidal curves were fit by the Hill equation, which provided the maximum level of phosphoenzyme (EP) formation and the [Ca^{2+}] required for half-maximum phosphoenzyme formation (K_{Ca}). EP levels are expressed in terms of nmol EP per nmol SERCA2a, according to the amount of SERCA2a per mg of Sf21 cell microsomes for each sample (Table 1). Samples were preincubated in the absence (−Ab) or presence (+Ab) of anti-phospholamban monoclonal antibody, 2D12, for 20 min on ice before the start of the phosphorylation experiments. Errors denote the spread of triplicate determinations for a single experiment using a single preparation of expressed protein. Experimental repeats using different preparations gave very similar results.

mum EP levels of ~0.075 nmol/nmol SERCA2a (Fig. 2 and Table 2). For comparison, similar experiments using dog cardiac SR (data not shown) revealed a maximum EP level of 0.21 nmol/mg SR, which was equivalent to 0.073 nmol/nmol SERCA2a. This result shows that the phosphorylation capacity of SERCA2a in the expressed samples was identical to that of native SERCA2a in cardiac SR. Thus the relatively low maximum EP levels reported here arose from the low, subsaturating [ATP] concentration utilized in the experiment (cf. Froehlich and Taylor, 1975; Tada et al., 1980) and not from inactive SERCA2a in the expressed samples.

Ca-ATPase expressed without phospholamban displayed a K_{ca} of 200 nM for steady-state EP formation, which was unaffected by treatment of these microsomes with 2D12 (Table 2). When SERCA2a was coexpressed with wild-type phospholamban, the K_{ca} value increased to 460 nM (ΔK_{Ca} = 210 nM relative to the antibody-treated sample). When coexpressed with the monomeric mutant L37A-phospholamban, the K_{ca} value increased to a greater extent to 800 nM (ΔK_{Ca} = 400 nM relative to the antibody-treated sample). For both phospholamban-coexpressed samples, treatment with 2D12 shifted the Ca^{2+} activation curve to the left, resulting in twofold decreased K_{Ca} values. As observed with measurement of steady-state ATPase activity at 37°C, the K_{Ca} value for the antibody-treated SERCA2a + wild-type phospholamban sample was not significantly different from that obtained for expression of SERCA2a in the absence of phospholamban. In contrast, the K_{Ca} value for the antibody-treated SERCA2a + L37A-phospholamban sample was greater than that of the SERCA2a alone sample, as was also observed for the 37°C steady-state activity measurements (Table 1). Similar to the effects of phospholamban on SERCA2a ATPase activity, treatment of each sample with anti-phospholamban antibody had no effect on the maximum steady-state EP levels formed, which were identical between all three sets of microsomes. Thus the results obtained for formation of steady-state EP levels at 0°C, using 1 μM ATP, mirrored the results obtained for measurement of steady-state ATP hydrolysis at 37°C using 5 mM ATP. Furthermore, the results show that the monomeric L37A-phospholamban mutant is a more potent inhibitor of SERCA2a steady-state phosphoenzyme formation than is wild-type phospholamban, but, in analogy to measurements of ATP hydrolysis (Autry et al., 1997; Kimura et al., 1997), even the more potent L37A-phospholamban does not affect the maximum SERCA2a steady-state EP level observed at saturating [Ca^{2+}].

In the next set of experiments, we measured the effect of phospholamban on the time course of EP formation by SERCA2a in Sf21 cell microsomes at 0°C (Fig. 3 and Table 3). These measurements were carried out for 268 nM $[Ca^{2+}]_{free}$, which is near the K_{Ca} value for each sample, and at a saturating Ca^{2+} level (15 μM $[Ca^{2+}]_{free}$), where phospholamban has no effect on Ca-ATPase activity (Fig. 2 and Table 1). At 268 nM $[Ca^{2+}]_{free}$ (Fig. 3, *left*), the EP formation time course for SERCA2a expressed alone (*top left*) exhibited a brief lag (with a time constant of 5 s^{-1}) followed by a monoexponential increase with a rate of 0.21 s^{-1}, and the steady-state phosphoenzyme level was 0.036 nmol EP/mg total protein (0.048 nmol EP/nmol SERCA2a). The presence of a lag phase in the EP formation time course is consistent with the fact that a series of kinetic steps precedes phosphoryl transfer from ATP to the enzyme (Frost and Pearson, 1953). Pretreatment of the sample with anti-phospholamban monoclonal antibody had no effect on the phosphoenzyme formation time course (Table 3). When coexpressed with wild-type phospholamban, the steady-state Ca-ATPase phosphoenzyme level (0.007 nmol EP/mg protein = 0.026 nmol EP/nmol SERCA2a) was decreased 33% relative to samples pretreated with anti-phospholamban monoclonal antibody (0.011 nmol EP/mg protein = 0.040 nmol EP/nmol SERCA2a), but neither the lag preceding EP formation (time constant of 1.8 s^{-1}) nor the apparent rate of EP formation (0.18 s^{-1}) was changed relative to the antibody-treated samples (0.18 s^{-1}). When coexpressed with the more potent monomeric L37A-phospholamban mutant, the steady-state Ca-ATPase phosphoen-

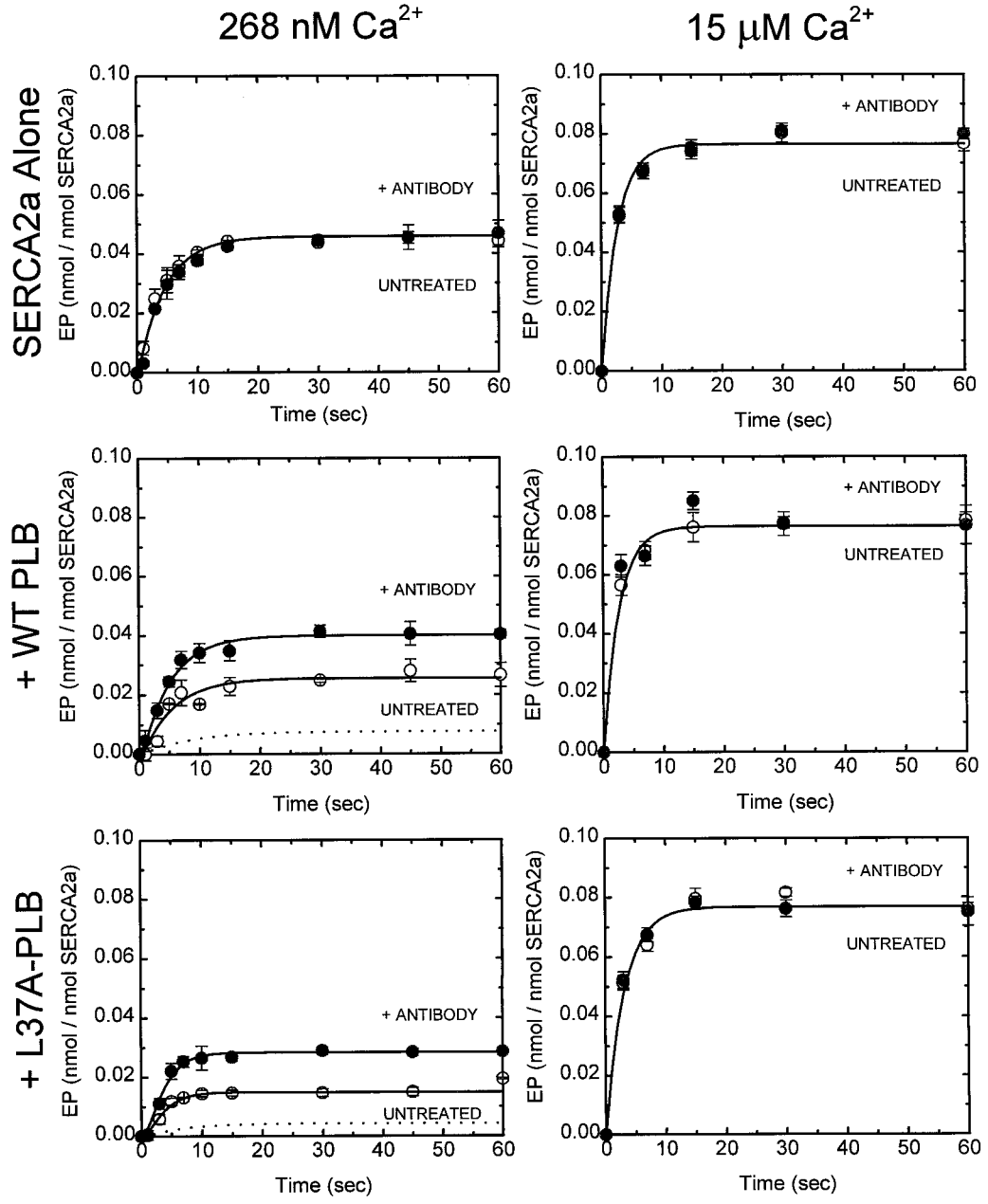

FIGURE 3 Time course of phosphoenzyme formation by SERCA2a in Sf21 microsomes by 1 μM ATP at 0°C. SERCA2a phosphorylation time courses were measured by adding 1 μM [γ-^{32}P]ATP and either 0.5 mM $CaCl_2$ (268 nM ionized Ca^{2+}, *left panels*) or 1.0 mM $CaCl_2$ (15 μM ionized Ca^{2+}, *right panels*) to Sf21 microsomes (0.1 mg/ml) preincubated in 1 mM EGTA (final conditions). The reaction was allow to proceed at 0°C for serial times as indicated, followed by acid quenching and processing as described in Materials and Methods. (*Top*) SERCA2a expressed alone; (*middle*) SERCA2a + wild-type phospholamban; (*bottom*) SERCA2a + L37A-phospholamban. Phosphorylation of SERCA2a in Sf21 microsomes pretreated with phospholamban monoclonal antibody, 2D12, are denoted by filled circles (●), and the control, untreated microsomes are denoted by the empty circles (○). The solid curves represent simulation of the EP formation time course, using the reactions of Scheme 3 and the rate constants in Table 6. The dotted curves represent simulations where the values of k_3 and k_{-3} (Table 6) were each decreased by a factor of 10. Symbols represent the average of triplicate measurements for a single preparation of each sample type. Error bars represent high and low values in each average. Additional experiments using different preparations provided equivalent results.

zyme level (0.006 nmol EP/mg protein = 0.016 nmol EP/nmol SERCA2a) was decreased by 45% relative to the sample pretreated with anti-phospholamban antibody (0.011 nmol EP/mg protein = 0.029 nmol EP/nmol SERCA2a), but again neither the lag preceding EP formation (time constant of 0.5 s^{-1}) nor the apparent rate of EP formation (0.22 s^{-1}) was changed relative to samples pretreated with anti-phospholamban monoclonal antibody (0.22 s^{-1}).

TABLE 3 SERCA2a phosphoenzyme formation fit parameters

	ionized $[Ca^{2+}]$				
	268 nM			15 μM	
	k_1 (s^{-1})	k_2 (s^{-1})	EP level (nmol/nmol SERCA2a)	k_1 (s^{-1})	EP level (nmol/nmol SERCA2a)
SERCA2a alone					
−Antibody	5.0 ± 1.0	0.21 ± 0.01	0.048 ± 0.001	0.38 ± 0.02	0.075 ± 0.001
+Antibody	5.0 ± 1.0	0.21 ± 0.01	0.048 ± 0.001	0.38 ± 0.02	0.075 ± 0.001
Ratio (+Ab/−Ab)	1.0	1.0	1.0	1.0	1.0
SERCA2a + WT-PLB					
−Antibody	1.8 ± 0.4	0.18 ± 0.02	0.026 ± 0.001	0.38 ± 0.01	0.076 ± 0.002
+Antibody	1.8 ± 0.4	0.18 ± 0.02	0.040 ± 0.001	0.38 ± 0.01	0.076 ± 0.002
Ratio (+Ab/−Ab)	1.0	1.0	1.5	1.0	1.0
SERCA2a + L37A-PLB					
−Antibody	0.5 ± 0.1	0.22 ± 0.01	0.016 ± 0.001	0.38 ± 0.01	0.077 ± 0.001
+Antibody	0.5 ± 0.1	0.22 ± 0.01	0.029 ± 0.001	0.38 ± 0.01	0.077 ± 0.001
Ratio (+Ab/−Ab)	1.0	1.0	1.8	1.0	1.0

Phosphoenzyme (EP) formation time courses measured at 268 nM ionized $[Ca^{2+}]$ (Fig. 3, *left*) were fit with a lag function (Frost and Pearson, 1953), $EP(t) = A_0(1 + A_1e^{-k1t} - A_2e^{-k2t})$, where A_0 is the amplitude (in nmol EP/nmol SERCA2a), k_1 is the time constant for the lag phase (in s^{-1}), k_2 is the rate of the monoexponential rise (in s^{-1}), $A_1 = k_2/(k_1 - k_2)$, and $A_2 = k_1/(k_1 - k_2)$. EP formation time courses measured at 15 μM ionized Ca^{2+} (Fig. 3, *right*) were fit with a single-exponential function, $EP(t) = A(1 - e^{-kt})$, where A is the amplitude (in nmol EP/nmol SERCA2a) and k is the rate (in s^{-1}). Initial values of A_i and k_i were obtained from semilog plots of the phosphoenzyme formation data but were allowed to vary freely during the fit. The only constraint imposed was a minimum value of zero for each parameter. EP levels are expressed in terms of nmol EP per nmol SERCA2a, according to the amount of SERCA2a per mg of Sf21 cell microsomes for each sample (Table 1). Errors denote the spread of triplicate determinations for a single experiment using a single preparation of expressed protein. Experimental repeats using different preparations of the same sample types gave very similar phosphoenzyme formation time courses.

At 15 μM $[Ca^{2+}]_{free}$ (Fig. 3, *right*), the apparent rate of EP formation (0.38 s^{-1}) and the steady-state EP level (0.076 nmol EP/nmol SERCA2a) were similar for each of the samples (Table 3). In addition, there was no discernible lag phase preceding EP formation for any of the expressed SERCA2a samples. Before the steady-state EP levels were adjusted for the amount of SERCA2a in each sample type, the steady-state EP levels were 0.055 nmol EP/mg protein for SERCA2a expressed alone, 0.021 nmol EP/mg protein for SERCA2a + wild-type phospholamban, and 0.030 nmol EP/mg for SERCA2a + L37A-phospholamban. Pretreatment of the three samples with anti-phospholamban monoclonal antibody had no effect on the rate of EP formation or the steady-state EP level (Table 3). Additional EP formation experiments, carried out at 625 nM $[Ca^{2+}]_{free}$ (not shown), produced results entirely similar to those obtained at 268 nM ionized $[Ca^{2+}]$. Phospholamban had no effect on the apparent rate of EP formation (0.26 s^{-1} for each sample, ± antibody treatment), but treatment of the phospholamban-containing samples with anti-phospholamban antibody resulted in a stimulation of the steady-state EP level of the wild-type phospholamban sample by 30% and of the more potent L37A-phospholamban sample by 70%. In summary, the results of the phosphoenzyme formation studies show that phospholamban does not affect the apparent rate of EP formation. Because the apparent rate of SERCA2a phosphorylation is directly controlled by the rate of the Ca-ATPase E1·Ca-to-E1′·Ca transition under the conditions of our experiments (Tada et al., 1980; Cantilina et al., 1993), the results do not support the hypothesis that phospholamban inhibits this transition in the SERCA2a cycle.

SERCA2a P_i liberation and phosphoenzyme decomposition

The second goal of our kinetics studies was to test the hypothesis that phospholamban inhibits Ca-ATPase cycling by decreasing the rate of EP decomposition (step 5, Scheme 1). To test this hypothesis, we measured the effect of phospholamban coexpression on the time course of P_i release (Fig. 4 and Table 4), concomitant with our EP formation experiments. This was accomplished by collecting an aliquot of the EP reaction mixture for each sample after the quenched membranes were pelletted. The unreacted radiolabeled ATP was removed from the sample by charcoal extraction, and the $^{32}P_i$ in the aliquot was separated by complexation with ammonium molybdate and extraction into organic solvent. The P_i liberation time courses for all samples at both 268 nM and 15 μM $[Ca^{2+}]_{free}$ exhibited a brief lag (~5–7 s), which coincided with the build-up of SERCA2a EP, followed by a linear increase in P_i over time during the steady-state phase of SERCA2a turnover. At 268 nM ionized $[Ca^{2+}]$, the rate of P_i liberation for SERCA2a

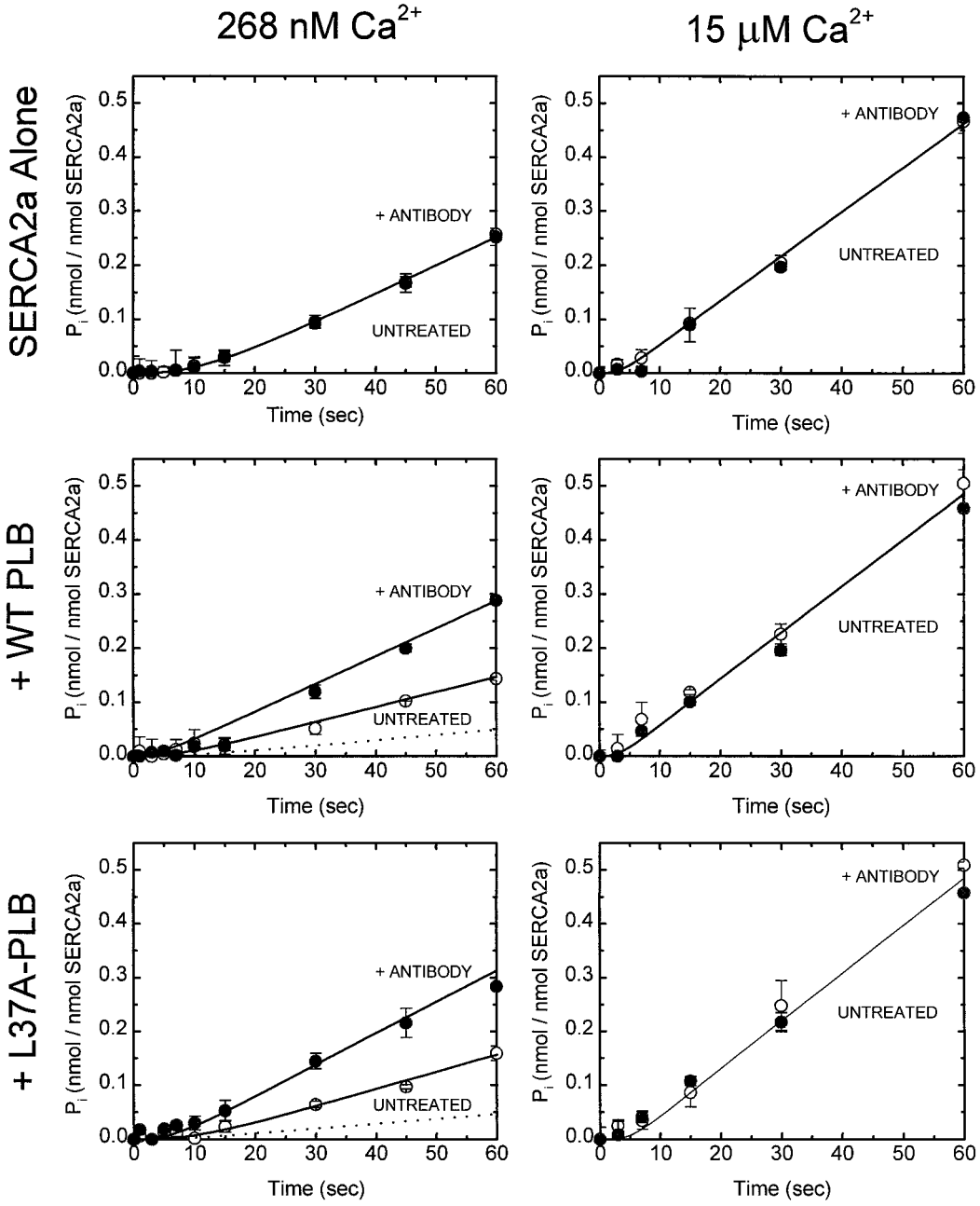

FIGURE 4 Time course of phosphate liberation by SERCA2a in Sf21 microsomes in the presence of 1 μM ATP at 0°C. SERCA2a phosphorylation time courses were measured as described in the legend of Fig. 3. Inorganic phosphate in each sample was isolated and processed as described in Materials and Methods. (*Top*) SERCA2a expressed alone; (*middle*) SERCA2a + wild-type phospholamban; (*bottom*) SERCA2a + L37A-phospholamban. Phosphorylation of SERCA2a in Sf21 microsomes pretreated with phospholamban monoclonal antibody, 2D12, is denoted by filled circles (●), and the control, untreated microsomes are denoted by the empty circles (○). The solid curves represent simulation of the P_i liberation time course, using the reactions of Scheme 3 and the rate constants in Table 6. The dotted curves represent simulations where the values of k_3 and k_{-3} (Table 6) were each decreased by a factor of 10. Symbols represent the average of triplicate measurements for a single preparation of each sample type (Table 4). Error bars represent high and low values in each average. Additional experiments using different preparations provided equivalent results.

expressed alone was 3.6×10^{-3} nmol P_i·mg protein^{-1}·s^{-1} (6.6×10^{-3} nmol P_i·nmol SERCA2a^{-1}·s^{-1}), and this rate was not affected by pretreatment of the sample with anti-phospholamban monoclonal antibody. When coexpressed with wild-type phospholamban, the rate of P_i liberation by SERCA2a (1.3×10^{-3} nmol P_i·mg protein^{-1}·s^{-1} or 4.5×10^{-3} nmol P_i·nmol SERCA2a^{-1}·s^{-1}) was decreased 33% relative to the sample pretreated with anti-phospholamban monoclonal antibody (2.0×10^{-3} nmol P_i·mg protein^{-1}·s^{-1} or 7.0×10^{-3} nmol P_i·nmol SERCA2a^{-1}·s^{-1}). When co-

TABLE 4 Steady-state P_i liberation fit parameters

	$[Ca^{2+}]_{free}$	
	268 nM rate (nmol P_i · nmol SERCA2a^{-1} · s^{-1})	15 μM rate (nmol P_i · nmol SERCA2a^{-1} · s^{-1})
SERCA2a alone		
−Antibody	0.0066 ± 0.0004	0.010 ± 0.005
+Antibody	0.0066 ± 0.0004	0.010 ± 0.005
Ratio (+Ab/−Ab)	1.0	1.1
SERCA2a + WT-PLB		
−Antibody	0.0045 ± 0.001	0.011 ± 0.001
+Antibody	0.0070 ± 0.001	0.011 ± 0.001
Ratio (+Ab/−Ab)	1.5	1.0
SERCA2a + L37A-PLB		
−Antibody	0.0044 ± 0.0008	0.015 ± 0.001
+Antibody	0.0080 ± 0.0008	0.0015 ± 0.001
Ratio (+Ab/−Ab)	1.8	1.0

Inorganic phosphate (P_i) liberation time courses (Fig. 4) were measured in conjunction with phosphoenzyme formation experiments (Fig. 3). The steady-state rate of P_i production was determined by fitting the linear phase (from 15 to 60 s) of the P_i liberation time course. P_i liberation rates are expressed in terms of nmol P_i · nmol SERCA2a^{-1} · s^{-1}, according to the amount of SERCA2a per mg of Sf21 cell microsomes for each sample (Table 1). Errors denote the spread of triplicate determinations for a single experiment using a single preparation of expressed protein. Experimental repeats using different preparations of the same sample type gave very similar P_i liberation curves.

expressed with the more potent monomeric L37A-phospholamban mutant, the rate of P_i liberation by SERCA2a (1.9×10^{-3} nmol P_i·mg protein^{-1}·s^{-1} or 4.5×10^{-3} nmol P_i·nmol SERCA2a^{-1}·s^{-1}) was decreased by 45% relative to the sample pretreated with anti-phospholamban antibody (3.3×10^{-3} nmol P_i·mg protein^{-1}·s^{-1} or 8.0×10^{-3} nmol P_i·nmol SERCA2a^{-1}·s^{-1}). At 15 μM $[Ca^{2+}]_{free}$, the rate of P_i liberation by SERCA2a in each of the expressed samples was unaffected by pretreatment with anti-phospholamban monoclonal antibody. When the raw P_i liberation rates (4.4×10^{-3} (SERCA2a), 5.3×10^{-3} (SERCA2a + wild-type phospholamban), and 5.9×10^{-3} (SERCA2a + L37A-phospholamban) nmol P_i·mg protein^{-1}·s^{-1}) were corrected for differences in Ca-ATPase expression levels in the different samples (Table 1), the three samples showed essentially the same rates: 0.010 (SERCA2a alone), 0.011 (SERCA2a + wild-type phospholamban) and 0.015 (SERCA2a + L37A-phospholamban) nmol P_i·nmol SERCA2a^{-1}·s^{-1} (Table 4). Thus, even for the enzyme at 0°C with micromolar ATP concentration, inhibition of overall ATP hydrolysis by phospholamban occurs only at subsaturating ionized Ca^{2+} concentrations, and there is no apparent V_{max} effect. Additional P_i liberation experiments, carried out at 625 nM $[Ca^{2+}]_{free}$ (not shown), produced results entirely similar to those obtained at 268 nM ionized $[Ca^{2+}]$. Treatment of the phospholamban-containing samples with anti-phospholamban antibody 2D12 stimulated the rate of P_i liberation by the wild-type phospholamban sample by 30% and that of the more potent L37A-phospholamban sample by 45%. Taken together, the results show that phospholamban inhibits the apparent rate of product formation by SERCA2a.

Correlation of the P_i liberation and EP formation data showed that phospholamban (both wild-type and L37A-phospholamban) inhibited the rate of P_i liberation to the same extent as the inhibition of the steady-state EP level in each sample. Because product formation (P_i) depends on the rate of EP decomposition and the concentration of EP in the steady state ($d[P_i]/dt = k \times [EP]$), it appeared that the phospholamban-mediated reduction in the rate of P_i production was due to the decreased steady-state level of EP induced by phospholamban. Alternatively, phospholamban could have inhibited the rate of EP decomposition, resulting in the reduced rate of P_i liberation. To distinguish further between these two possibilities, we measured the effect of phospholamban on the rate of SERCA2a phosphoenzyme decomposition (Fig. 5). In this experiment, SERCA2a was phosphorylated with 1 μM ATP for 30 s at 0°C, which was sufficient time for the system to attain steady-state EP levels (Fig. 3). At 30 s, 5 mM EGTA (final concentration) was added to the reaction mixture to remove all traces of ionized Ca^{2+} from the reaction mixture and thus to stop SERCA2a phosphorylation by ATP. The phosphoenzyme present at the time of the EGTA addition decayed with an exponential time course, which was followed by quenching of the decay reaction at serial times after EGTA addition.

Fig. 5 shows the effect of phospholamban on the time course of EP decomposition by SERCA2a in Sf21 cell microsomes at 0°C. The decomposition time course for all samples was best fit by a monoexponential function. For each sample at each $[Ca^{2+}]$, the EP level at the zero time of the EP decay time course corresponded to the steady-state EP level measured in the EP formation experiments (Fig. 3 and Table 3). For phosphoenzyme formed at 268 nM $[Ca^{2+}]_{free}$, the apparent rate of EP decomposition in zero ionized Ca^{2+} was similar for all of the SERCA2a samples, 0.12 s^{-1} for SERCA2a expressed alone, 0.15 s^{-1} for SERCA2a + wild-type phospholamban, and 0.14 s^{-1} for SERCA2a + L37A-phospholamban (Table 5). Pretreatment of the samples with anti-phospholamban monoclonal antibody had no effect on the rate of phosphoenzyme decay. Additional experiments in which phosphoenzyme was formed at 15 μM $[Ca^{2+}]_{free}$ (Fig. 5 and Table 5) or 625 nM $[Ca^{2+}]_{free}$ (not shown), but at which phosphoenzyme decay proceeded at zero ionized Ca^{2+}, produced similar results. The EP decomposition rate was nearly identical for all samples (0.15 s^{-1} at 625 nM $[Ca^{2+}]_{free}$ and 0.20 s^{-1} 15 μM $[Ca^{2+}]_{free}$), and the rate was not affected by pretreatment with anti-phospholamban antibody. These results show that phospholamban does not alter the rate of SERCA2a phosphoenzyme decomposition occurring in the absence of significant ionized Ca^{2+}. Thus we conclude that phospholam-

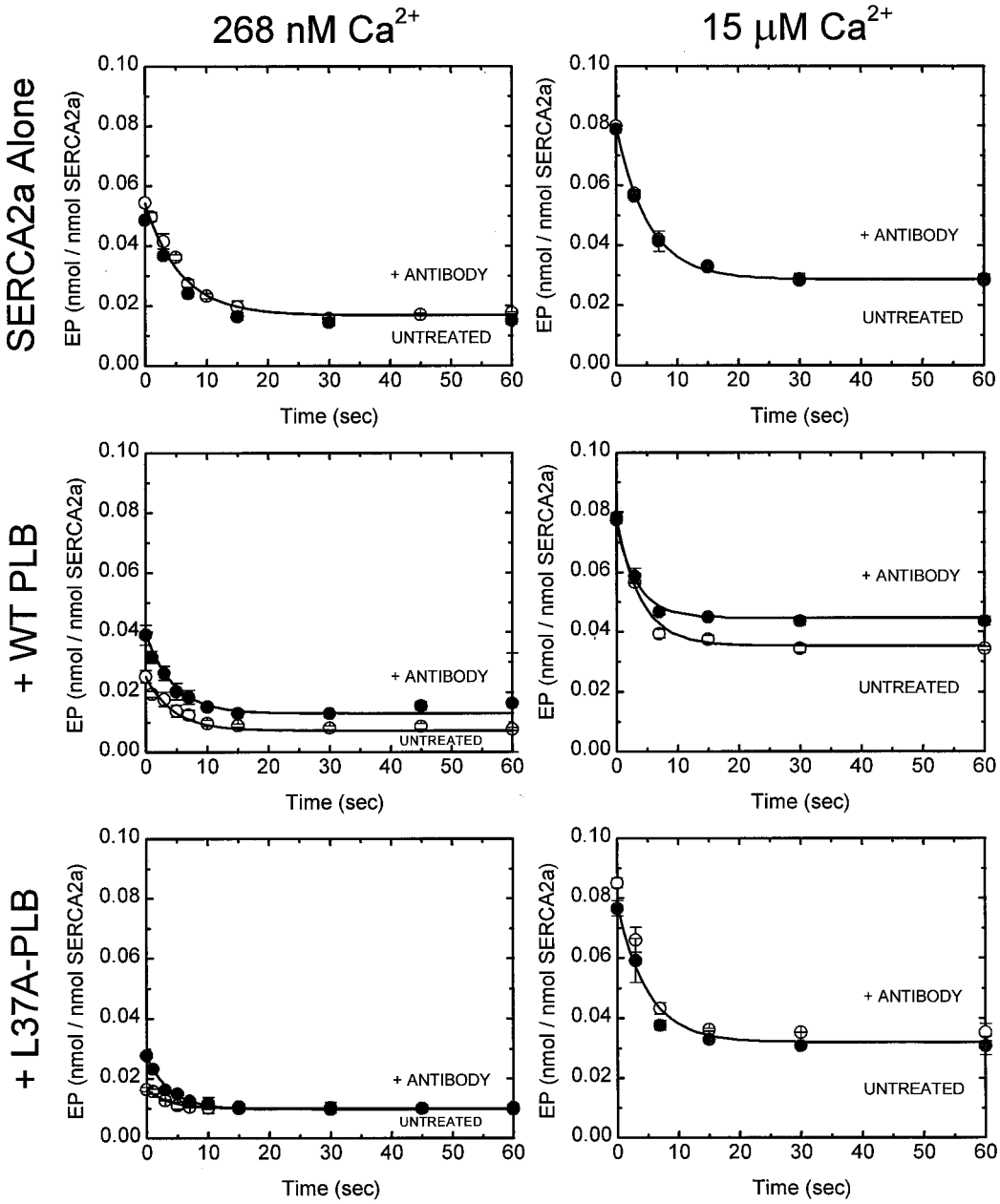

FIGURE 5 Time course of phosphoenzyme decomposition by SERCA2a in Sf21 microsomes after a 5 mM EGTA chase at 0°C. SERCA2a in Sf21 microsomes (0.1 mg/ml) preincubated in 1 mM EGTA was phosphorylated by 1 μM [γ-^{32}P]ATP and either 0.5 mM $CaCl_2$ (268 nM ionized Ca^{2+}, *left panels*) or 1.0 mM $CaCl_2$ (15 μM ionized Ca^{2+}, *right panels*) at 0°C (final conditions). After 30 s of phosphorylation, 5 mM EGTA (final) was added to the reaction to halt subsequent EP formation, and the decay of radiolabeled EP at 0°C was monitored by acid quenching the sample at serial times as indicated. The samples were processed as described in Materials and Methods. (*Top*) SERCA2a expressed alone; (*middle*) SERCA2a + wild-type phospholamban; (*bottom*) SERCA2a + L37A-phospholamban. Phosphoenzyme decomposition of SERCA2a in Sf21 microsomes pretreated with phospholamban monoclonal antibody, 2D12, is denoted by filled circles (●), and the control, untreated microsomes are denoted by empty circles (○). The solid curves represent simulation of the EP decay time course, using the reactions of Scheme 3 and the rate constants in Table 6. Symbols represent the average of triplicate measurements for a single preparation of each sample type. Error bars represent high and low values in each average. Additional experiments using different preparations provided equivalent results.

ban does not inhibit the rate of EP decay. Therefore, phospholamban inhibits P_i liberation as a consequence of the phospholamban-dependent reduction of steady-state SERCA2a EP levels, rather than by directly inhibiting the rate of EP decay.

Simulation of SERCA2a kinetics data

To determine the kinetic step(s) in the Ca-ATPase cycle affected by phospholamban that would result in a decreased steady-state EP level but no change in the rate of EP

TABLE 5 Phosphoenzyme decomposition rate constants

	$[Ca^{2+}]_{free}$	
	268 nM rate (s^{-1})	15 μM rate (s^{-1})
SERCA2a alone		
−Antibody	0.12 ± 0.02	0.19 ± 0.04
+Antibody	0.12 ± 0.02	0.19 ± 0.04
SERCA2a + WT-PLB		
−Antibody	0.15 ± 0.02	0.20 ± 0.03
+Antibody	0.15 ± 0.02	0.20 ± 0.03
SERCA2a + L37A-PLB		
−Antibody	0.14 ± 0.03	0.20 ± 0.02
+Antibody	0.14 ± 0.03	0.20 ± 0.02

Phosphoenzyme decomposition curves in Fig. 5 were fit with a single-exponential function, $EP(t) = Ae^{-kt}$, where A is the amplitude (in nmol EP/nmol SERCA2a) and k is the rate (in s^{-1}). Initial values of A and k were obtained from semilog plots of the phosphoenzyme decomposition data but were allowed to vary freely during the fit. The only constraint imposed was a minimum value of zero for each parameter. Errors denote the spread of triplicate determinations for a single experiment using a single preparation of expressed protein. Experimental repeats using different preparations gave very similar phosphoenzyme formation time courses.

formation or decay, the $[Ca^{2+}]$-dependent steady-state EP level and the time courses of EP formation, P_i liberation, and EP decay for each sample were simulated using the reactions of Scheme 3 and the rate constants presented in Table 6. The details of the simulations are presented in Materials and Methods. We first simulated the EP formation and P_i liberation time courses measured for the SERCA2a alone sample (Figs. 3 and 4, *top, solid lines*), to generate a set of rate constants that described the SERCA2a reaction cycle in the absence of phospholamban (Table 6). The best simulation of the data was obtained using a catalytic site density of 0.08 nmol/mg protein (0.11 nmol/nmol SERCA2a), based on the maximum amount of EP formed at saturating Ca^{2+} by the subsaturating, 1 μM ATP concentration used in the experiments. In the simulations, the rate of EP formation was dependent primarily on the forward rate of the E1·Ca-to-E1′·Ca transition (step 3), whereas the steady-state EP level was dependent both on the forward and reverse rates (i.e., the equilibrium constant) of the first Ca^{2+} ion binding to E1 (step 2) and the forward rate of the

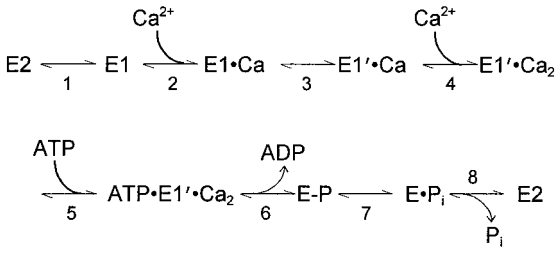

Scheme 3

TABLE 6 Kinetic constants for simulation of steady-state EP levels and EP formation and P_i liberation time courses of SERCA2a expressed alone in Sf21 insect cell microsomes

Reaction step of Scheme 3	Rate constants
k_1/k_{-1}	0.35 s^{-1}/0.35 s^{-1}
k_2/k_{-2}	2×10^8 M^{-1} s^{-1}/120 s^{-1}
k_3/k_{-3}	0.4 s^{-1}/0.4 s^{-1}
k_4/k_{-4}	8×10^7 M^{-1} s^{-1}/3.2 s^{-1}
k_5/k_{-5}	4×10^6 M^{-1} s^{-1}/0
k_6/k_{-6}	35 s^{-1}/0
k_7/k_{-7}	0.3 s^{-1}/0.7 s^{-1}
k_8/k_{-8}	0.5 s^{-1}/0

Rate constants for the reaction mechanism shown in Scheme 3 were evaluated by simulation of the $[Ca^{2+}]$ dependence of steady-state phosphoenzyme (EP) levels (Fig. 2) and the EP formation (Fig. 3) and P_i liberation (Fig. 4) time courses, using the program KINSIM (Barshop et al., 1983). All rate constants were allowed to vary freely during the simulation, with the exception that a minimum value of zero was imposed for each rate. Additional details for the simulations are provided in the text.

E1·Ca-to-E1′·Ca transition (step 3). The rate of the E2-to-E1 transition (step 1) had only minor effects on the EP formation time course, provided the rate of k_1 remained greater than 0.1 s^{-1}. At lower values of k_1, the simulated EP formation did not fit the experimental data. The rate of the second Ca^{2+} ion binding to E1′·Ca (step 4), the rate of ATP binding to E1′·Ca_2 (step 5), and the rate of phosphoryl transfer from ATP to the enzyme (step 6) had little influence on the simulations, because the rates of these steps were much faster than the adjacent slow steps (steps 3 and 7). The rates of EP decomposition and P_i release (steps 7 and 8) were selected to allow the phosphoenzyme to rise to its steady-state level without passing through an "overshoot," while simultaneously matching the lag and linear phases of the P_i liberation time course. Some minor adjustments in steps 7 and 8 were required to produce a more precise simulation of the steady-state phase of EP formation and P_i liberation at each ionized $[Ca^{2+}]$ studied, but the selected rates for steps 7 and 8 were verified by simulating the SERCA2a alone EP decay data at each Ca^{2+} level (Fig. 5, *top, solid lines*). By carrying out the same simulation at a series of ionized $[Ca^{2+}]$ between 0 and 15 μM, the $[Ca^{2+}]$ dependence of the steady-state EP levels were accurately reproduced (Fig. 2, *solid symbols*). This result validated Scheme 3 and the kinetic constants of Table 6 as an appropriate model for simulating SERCA2a kinetics under our experimental conditions and for elucidating the effect of phospholamban on the SERCA2a reaction cycle.

Simulation of the kinetics data from the SERCA2a + wild-type phospholamban and SERCA2a + L37A-phospholamban microsomes (Figs. 3–5, *solid lines*) was carried out using a catalytic site density of 0.04 nmol/mg for the SERCA2a + wild-type phospholamban microsomes and 0.07 nmol/mg for the SERCA2a + L37A-phospholamban microsomes. The antibody-treated SERCA2a + wild-type

phospholamban and SERCA2a + L37A-phospholamban kinetics data (Figs. 3 and 4, *solid lines*) was simulated using the same kinetics constants used for the expressed SERCA2a microsomes, except that for the SERCA2a + L37A-phospholamban microsomes it was necessary to reduce by twofold the forward rate (k_2) of step 2 (Ca^{2+} binding to E1) to 1×10^8 M^{-1} s^{-1}, to properly reproduce the rate and amplitude of the EP formation and P_i liberation time courses. Similar to the SERCA2a alone sample, some minor adjustments for steps 7 and 8 were required to produce a precise simulation of the EP formation and P_i liberation time courses measured at the various ionized [Ca^{2+}] studied, but the selected rates for steps 7 and 8 were verified by simulating the EP decay data at each Ca^{2+} level (Fig. 5, *solid lines*). Finally, by carrying out the simulations at a series of ionized [Ca^{2+}] levels between 0 and 15 μM, the [Ca^{2+}] dependence of the steady-state EP levels for both antibody-treated samples were accurately reproduced (Fig. 2, *solid symbols*).

Two approaches were used to simulate the effect of coexpressed phospholamban on SERCA2a kinetics data obtained at 268 nM ionized [Ca^{2+}] (Figs. 3 and 4). First, we tested the proposal by Cantilina et al. (1993) that phospholamban decreases the forward and reverse rates of the E1·Ca-to-E1′·Ca transition (step 3, Scheme 3) by 10-fold. Changing k_3 and k_{-3} from 0.4 s^{-1} to 0.04 s^{-1} resulted in EP formation (Fig. 3, *left, dashed lines*) and P_i liberation (Fig. 4, *left, dashed lines*) time courses that did not fit the data obtained from the two phospholamban-containing samples. Similar results were obtained when the untreated kinetics data obtained at 625 nM (not shown) were simulated, and even at saturating [Ca^{2+}] (also not shown), where there should be no difference between untreated and antibody-treated data (Figs. 3–5). Therefore, the results of this approach suggest that phospholamban does not inhibit SERCA2a EP formation by inhibiting the E1·Ca-to-E1′·Ca transition.

We next focused on Ca^{2+} binding to E1 (step 2, Scheme 3) as a target for phospholamban inhibition, because our simulations showed that the kinetic constants for this step had substantial effects on the steady-state EP level but only minor effects on the rate of EP formation in the simulations (see above). For both the SERCA2a + wild-type phospholamban and the SERCA2a + L37A-phospholamban kinetics data, a twofold decrease in the equilibrium constant (K_{eq}) for step 2 was sufficient, by itself, to simulate the untreated EP formation and P_i liberation time courses at both 268 nM (Figs. 3 and 4, *left, solid lines*) and 625 nM (not shown) ionized [Ca^{2+}]. For the SERCA2a + wild-type phospholamban microsomes, k_2 was reduced to 1×10^8 M^{-1} s^{-1}, whereas for the SERCA2a + L37A-phospholamban microsomes, k_2 was reduced to 5×10^7 M^{-1} s^{-1}. (The same result was achieved by holding k_2 constant and increasing k_{-2} by a factor of 2 to 240 s^{-1} for both samples.) At 15 μM ionized Ca^{2+}, the twofold decrease in k_2 had no effect on the simulated kinetics; the EP formation, P_i liberation, and EP decay time courses generated were identical to the simulations of the antibody-treated data. This result was validated by conducting the simulation at a series of ionized [Ca^{2+}], which accurately reproduced the [Ca^{2+}] dependence of the steady-state EP levels measured for both untreated samples (Fig. 2, *solid symbols*). Thus the results of the simulations show that wild-type phospholamban inhibits SERCA2a by decreasing by twofold the equilibrium binding of the first Ca^{2+} to E1 relative to the SERCA2a alone sample. L37A-phospholamban is more potent than wild-type phospholamban, because it decreases equilibrium Ca^{2+} binding to E1 by fourfold relative to the SERCA2a alone sample. Nevertheless, high ionized [Ca^{2+}] is capable of reversing the inhibitory effect of phospholamban on SERCA2a completely, even the inhibition by the more potent L37A-phospholamban mutant.

DISCUSSION

In the present study, we have measured the effects of phospholamban on the time course of Ca-ATPase phosphorylation by ATP, to test the hypothesis (Cantilina et al., 1993) that phospholamban inhibits Ca-ATPase cycling by decreasing by 10-fold the rate of the E1·Ca-to-E1′·Ca transition (Scheme 2). Likewise, we have measured the effects of phospholamban on the time courses of inorganic phosphate (P_i) liberation and phosphoenzyme (EP) decomposition, to test the hypothesis that phospholamban inhibits steady-state ATPase activity by decreasing the rate of SERCA2a EP decay. To assist in this work, we have made use of the baculovirus-Sf21 insect cell expression system (Autry and Jones, 1997) to produce microsomes containing 1) Ca-ATPase alone, 2) Ca-ATPase coexpressed with wild-type phospholamban, and 3) Ca-ATPase coexpressed with the monomeric L37A-phospholamban mutant (L37A-phospholamban). To further define the specific effects of phospholamban on SERCA2a kinetics, we used a monoclonal antibody against phospholamban to reverse phospholamban inhibitory effects. The expressed SERCA2a samples had the same specific ATPase activity as SERCA2a in dog cardiac SR, and the SERCA2a in the expressed samples was phosphorylated to the same extent as SERCA2a in dog cardiac SR. The inhibitory effects of wild-type phospholamban on SERCA2a in the expressed sample were nearly identical to those measured for cardiac SR, and pretreatment with anti-phospholamban antibody relieved the inhibition to the same extent in the two samples. Because of the relatively high levels of SERCA2a and phospholamban expression provided by the baculovirus-Sf21 insect cell expression system, we were able to measure the effects of phospholamban on the phosphorylation and dephosphorylation kinetics of the expressed SERCA2a for the first time. Furthermore, the yield of SERCA2a from a single preparation provided sufficient material to carry out all of the experiments shown

here for each sample type. This is advantageous, because the results from several different types of kinetics experiments can be compared directly without having to correct for individual preparation differences. Our kinetics studies corroborate previous reports (Autry and Jones, 1997; Kimura et al., 1997) that L37A-phospholamban is a more potent inhibitor of the Ca-ATPase than wild-type phospholamban. At low ionized [Ca^{2+}] (268 nM and 625 nM), we found that L37A-phospholamban decreased the steady-state EP level and the apparent rate of P_i liberation to a greater extent (45%) than did wild-type phospholamban (33%). Despite being the more potent regulator, L37A-phospholamban, like wild-type phospholamban, did not affect the rates of SERCA2a EP formation or decomposition relative to SERCA2a in the absence of phospholamban. The results of our steady-state EP level studies also confirm the findings of other reports (Kranias, 1985; Cantilina et al., 1993; Autry and Jones, 1997; Chu et al., 1998) that phospholamban, even the more potent L37A-phospholamban mutant, does not affect SERCA2a V_{max} or the maximum steady-state EP levels at saturating [Ca^{2+}].

A number of investigators (Tada et al., 1979; Antipenko et al., 1997a, 1999) have reported that phospholamban inhibits SERCA2a by decreasing the rate of phosphoenzyme hydrolysis (step 5, Scheme 1). Most of these studies, however, were done with dog cardiac SR, in which phospholamban was always present and in which phospholamban inhibitory effects had to be reversed by phospholamban phosphorylation. Our EP decomposition results, obtained with a more controllable system, disagree with these reports, showing that phospholamban, even the more potent L37A-phospholamban mutant, does not affect the rate of EP decomposition. This may be due, in part, to the significant differences in reaction conditions (temperature, [ATP], [Ca^{2+}], etc.) between our kinetics studies and previous reports. Of these differences, the [ATP] may be the most important, because high ATP concentrations have been suggested to increase the rate of EP decomposition and turnover (Inesi, 1985), and McKenna and co-workers (McKenna et al., 1996; Coll et al., 1999) have demonstrated a relationship between nucleotide activation of SERCA2a and phospholamban regulation of SERCA2a activity. However, it is unlikely that our reaction conditions prevented us from observing an effect of phospholamban on the rate of SERCA2a EP decomposition. Phosphoenzyme decomposition reduces steady-state EP levels by reducing the number of phosphorylated enzymes. If phospholamban inhibits the rate of EP decomposition, we would expect to observe a greater fraction of phosphorylated enzymes during steady-state enzyme cycling—hence increased steady-state phosphoenzyme levels, when phospholamban is regulatory relative to samples pretreated with anti-phospholamban antibody to remove phospholamban inhibition. This clearly was not the case. Rather, we found that phospholamban decreased the SERCA2a steady-state EP level and, as a result, reduced the rate of P_i production to the same extent. Therefore, we conclude that phospholamban shifts the [Ca^{2+}] dependence of P_i production (i.e., ATPase activity) by a similar shift in the [Ca^{2+}] dependence of steady-state EP levels (as described below), and not by affecting the rate of EP decay. This conclusion is best supported by our finding of nearly identical effects of phospholamban on the [Ca^{2+}] dependence of steady-state EP levels and ATPase activity.

A number of other investigators (Cantilina et al., 1993; Negash et al., 1996; Antipenko et al., 1997a) have proposed that phospholamban inhibits Ca-ATPase cycling by increasing the activation energy of the E1·Ca-to-E1′·Ca conformational change (Scheme 2). Our EP formation studies were designed to quantitatively test this proposal as follows. The Ca-ATPase was preincubated in 1 mM EGTA to remove all traces of Ca^{2+} from the medium and thereby stabilize the enzyme in a Ca^{2+}-free state. At time 0, ATP and $CaCl_2$ were simultaneously added to the enzyme, and the apparent rate of ATP-dependent phosphorylation was measured. Under these conditions, Ca^{2+} must first bind to the Ca-ATPase E1 intermediate and stimulate the formation of the E1′·Ca_2 intermediate before ATP-dependent phosphorylation can occur (Scheme 2). According to Cantilina et al. (1993), the E1·Ca-to-E1′·Ca transition (step 2, Scheme 2) is the rate-determining step preceding phosphoryl transfer from ATP to the enzyme (see figure 10 of Cantilina et al., 1993), such that the apparent rate of SERCA2a phosphorylation should be determined largely by the rate of this transition. Therefore, if phospholamban decreases the rate of the E1·Ca-to-E1′·Ca transition by 10-fold, we would expect to observe a clear difference in the apparent rate of phosphoenzyme formation between the control samples and samples pretreated with a monoclonal antibody against phospholamban, 2D12, which uncouples phospholamban from the Ca-ATPase. However, our results did not support this. Our EP formation data at 268 nM ionized Ca^{2+} (Fig. 3 and Table 3) and 625 nM ionized Ca^{2+} (not shown) indicated no difference in the apparent rate of EP formation before or after antibody treatment. Thus we conclude that phospholamban does not inhibit Ca-ATPase cycling by decreasing the rate of the E1·Ca-to-E1′·Ca transition.

Additional evidence to rule out a phospholamban effect on the SERCA2a E1·Ca-to-E1′·Ca transition was provided by our simulations. Similar to the results of Cantilina et al. (1993), the rate of the E1·Ca-to-E1′·Ca transition in our model (Scheme 3 and Table 6) limits the rate of EP formation and the steady-state EP level. Because the rates of EP breakdown and the E2-to-E1 transition are similar to that of the E1·Ca-to-E1′·Ca transition, phosphoenzyme is formed at about the same rate that it decays, giving rise to the observed steady-state EP level. However, decreasing k_3 and k_{-3} by 10-fold makes the rate of EP formation much slower than the rate of EP decay, resulting in very low steady-state EP levels, with concomitantly low rates of P_i liberation (Fig.

3 and 4, *dashed lines*). Even at saturating (15 μM) ionized [Ca^{2+}], a 10-fold decrease in the bidirectional rate of step 3 dramatically slows the rate of EP formation and decreases the steady-state EP level (not shown). These changes clearly do not match the observed effects of phospholamban on SERCA2a kinetics. Therefore, our simulations corroborate the conclusion that phospholamban does not inhibit Ca-ATPase cycling by decreasing the rate of the E1·Ca-to-E1′·Ca transition.

In contrast, our simulations indicated that phospholamban inhibits SERCA2a activity by decreasing the equilibrium binding of the first Ca^{2+} to E1 (step 2, Scheme 3). Proper simulation of our kinetics data was obtained using $k_2 = 2 \times 10^8\ M^{-1}\ s^{-1}$ and $k_{-2} = 120\ s^{-1}$, resulting in an equilibrium constant for the first Ca^{2+} binding ($K_{eq,\ 2}$; step 2) of $1.66 \times 10^6\ M^{-1}$, and $k_4 = 8 \times 10^7\ M^{-1}\ s^{-1}$ and $k_{-4} = 3.2\ s^{-1}$, resulting in an equilibrium constant for the second Ca^{2+} binding ($K_{eq,\ 4}$; step 4) of $2.5 \times 10^7\ M^{-1}$. Therefore, the equilibrium constant for the second Ca^{2+} binding was larger than that for the first Ca^{2+} binding, which satisfied the condition for positive cooperativity of Ca^{2+} binding. At all ionized [Ca^{2+}] levels studied, Ca^{2+} was in great excess over the concentration of enzyme, allowing us to consider the forward reactions of steps 2 and 4 in pseudo-first-order terms. For example, at 268 nM ionized [Ca^{2+}], k_2' was 54 s^{-1}, resulting in an effective $K_{eq,\ 2}'$ of 0.45, and k_4' was 21 s^{-1}, resulting in an effective $K_{eq,\ 4}'$ of 6.6. As such, the amount of E1′·Ca_2 available for phosphorylation by ATP (i.e., the steady-state EP level) was controlled largely by the equilibrium of step 2, which favored Ca^{2+} dissociation from the enzyme. Thus, by imposing a twofold decrease in the affinity of SERCA2a for the first Ca^{2+}, phospholamban effectively reduced the amount of enzyme that was catalytically activated (E1′·Ca_2) to split ATP and transport Ca^{2+}. This accounts for the greater potency of L37A-phospholamban as a SERCA2a inhibitor than wild-type phospholamban, because L37A-phospholamban reduces the Ca^{2+} binding equilibrium to a greater extent (fourfold) than does wild-type phospholamban (twofold). In contrast, at 15 μM ionized [Ca^{2+}], k_2' was 3000 s^{-1}, resulting in an effective $K_{eq,\ 2}'$ of 25, and k_4' was 1200 s^{-1}, resulting in an effective $K_{eq,\ 4}'$ of 375. Under these conditions, a two- or fourfold decrease in SERCA2a affinity for the first Ca^{2+} imposed by phospholamban or L37A-phospholamban, respectively, would have no effect on SERCA2a kinetics, because the equilibrium would still strongly favor the formation of E1·Ca. Thus at high ionized [Ca^{2+}], phospholamban would not have any influence over SERCA2a kinetics. These effects are entirely consistent with the well-documented inhibition of SERCA2a by phospholamban; phospholamban decreases the apparent Ca^{2+} affinity of SERCA2a and inhibits the enzyme at low ionized [Ca^{2+}] levels, but not at saturating [Ca^{2+}]. Therefore, we conclude that phospholamban inhibits SERCA2a by decreasing SERCA2a affinity for Ca^{2+}.

Our studies show that the quintessence of the phospholamban effect on the Ca-ATPase is to lower the apparent affinity of the enzyme for Ca^{2+}. Paradoxically, however, when enzyme affinity for Ca^{2+} was measured directly under steady-state conditions in the previous study by Cantilina et al. (1993), no effect of phospholamban on Ca^{2+} affinity was detected. However, Cantilina et al. measured Ca^{2+} binding to the Ca-ATPase under passive conditions (i.e., in the absence of ATP and Mg), in which the enzyme was not hydrolyzing ATP and not actively transporting Ca^{2+}. Our results presented here make the novel prediction that equilibrium Ca^{2+} binding to the enzyme would be decreased by phospholamban interaction with the Ca-ATPase, if the measurement were to be made under conditions in which the enzyme was actively transporting Ca^{2+}. Experiments are currently in progress to test the hypothesis that phospholamban lowers equilibrium Ca^{2+} binding to the Ca-ATPase, but only under the condition in which the enzyme is hydrolyzing ATP and actively transporting Ca^{2+}.

We gratefully acknowledge the technical assistance of Jeff Kelley and Jamie Huffman. Samantha Gadd, Jason Southall, and Eddie Ebert assisted with the phosphoenzyme formation experiments during a research rotation with JEM. We thank Dr. John Durham for the use of his cell culture facilities. We thank Dr. Jeffrey Froehlich for substantial help with the kinetics simulations and for critically evaluating the manuscript.

This work was supported by the American Heart Association, WV-OH Affiliate (grant-in-aid WV-97-07-B to JEM), and the National Institutes of Health (grant HL49428 to LRJ).

REFERENCES

Antipenko, A. Y., A. I. Spielman, and M. A. Kirchberger. 1997a. Comparison of the effects of phospholamban and jasmone on the calcium pump of cardiac sarcoplasmic reticulum. *J. Biol. Chem.* 272:2852–2860.

Antipenko, A., A. I. Spielman, and M. A. Kirchberger. 1999. Kinetic differences in the phospholamban-regulated calcium pump when studied in crude and purified cardiac sarcoplasmic reticulum vesicles. *J. Membr. Biol.* 167:257–265.

Antipenko, A., A. I. Spielman, M. Sassaroli, and M. A. Kirchberger. 1997b. Comparison of the kinetic effects of phospholamban phosphorylation and anti-phospholamban monoclonal antibody on the calcium pump in purified cardiac sarcoplasmic reticulum membranes. *Biochemistry.* 36:12903–12910.

Autry, J. M., and L. R. Jones. 1997. Functional coexpression of the canine cardiac Ca^{2+} pump and phospholamban in *Spodoptera frugiperda* (Sf21) cells reveals new insights on ATPase regulation. *J. Biol. Chem.* 272:15872–15880.

Autry, J. M., and L. R. Jones. 1998. High-level co-expression of the canine cardiac calcium pump and phospholamban in Sf21 insect cells. *Ann. N.Y. Acad. Sci.* 853:92–102.

Barshop, B. A., R. F. Wrenn, and C. Frieden. 1983. Analysis of numerical methods for computer simulation of kinetic processes: development of KINSIM—a flexible, portable system. *Anal. Biochem.* 130:134–145.

Briggs, F. N., K. F. Lee, A. W. Wechsler, and L. R. Jones. 1992. Phospholamban expressed in slow-twitch and chronically stimulated fast-twitch muscle minimally affects calcium affinity of sarcoplasmic reticulum Ca^{2+}-ATPase. *J. Biol. Chem.* 267:26056–26061.

Cantilina, T., Y. Sagara, G. Inesi, and L. R. Jones. 1993. Comparative studies of cardiac and skeletal sarcoplasmic reticulum ATPases. *J. Biol. Chem.* 268:17018–17025.

Chu, G., L. Li, Y. Sato, J. M. Harrer, V. J. Kadambi, B. D. Hoit, D. M. Bers, and E. G. Kranias. 1998. Pentameric assembly of phospholamban facilitates inhibition of cardiac function in vivo. *J. Biol. Chem.* 273: 33674–33680.

Coll, K. E., R. G. Johnson, Jr., and E. McKenna. 1999. Relationship between phospholamban and nucleotide activation of cardiac sarcoplasmic reticulum Ca^{2+} adenosine triphosphatase. *Biochemistry.* 38: 2444–2451.

Froehlich, J. P., and E. W. Taylor. 1975. Transient state kinetic studies of sarcoplasmic reticulum adenosine triphosphatase. *J. Biol. Chem.* 250: 2013–2021.

Froehlich, J. P., and E. W. Taylor. 1976. Transient state kinetic effects of calcium ion on sarcoplasmic reticulum adenosine triphosphatase. *J. Biol. Chem.* 251:2307–2315.

Frost, A. A., and R. G. Pearson. 1953. Kinetics and Mechanism. Chap. 8. John Wiley and Sons, New York. 147–190.

Fujii, J., A. Ueno, K. Kitano, S. Tanaka, M. Kadoma, and M. Tada. 1987. Complete complementary DNA-derived amino acid sequence of canine cardiac phospholamban. *J. Clin. Invest.* 79:301–304.

Harrison, S. M., and Don M. Bers. 1989. Correction of proton and Ca association constants of EGTA for temperature and ionic strength. *Am. J. Physiol.* 256:C1250–C1256.

Hughes, G., J. M. East, A. G. Lee. 1994. The hydrophilic domain of phospholamban inhibits the Ca^{2+} transport step of the Ca^{2+}-ATPase. *Biochem. J.* 303:511–516.

Inesi, G. 1985. Mechanism of calcium transport. *Annu. Rev. Physiol.* 47:573–601.

Inesi, G., M. Kurzmack, C. Coan, and D. Lewis. 1980. Cooperative calcium binding and ATPase activation in sarcoplasmic reticulum vesicles. *J. Biol. Chem.* 255:3025–3031.

Jones, L. R., H. R. Besch, Jr., and A. M. Watanabe. 1978. Regulation of the calcium pump of cardiac sarcoplasmic reticulum. *J. Biol. Chem.* 251: 1643–1653.

Jones, L. R., and L. J. Field. 1993. Residues 2–25 of phospholamban are insufficient to inhibit Ca^{2+} transport ATPase of cardiac sarcoplasmic reticulum. *J. Biol. Chem.* 268:11486–11488.

Jones, L. R., S. H. Phan, and H. R. Besch, Jr. 1979. Gel electrophoretic and density gradient analysis of the (K^+ + Ca^{2+})-ATPase and the (Na^+ + K^+)-ATPase activities of cardiac membrane vesicles. *Biochim. Biophys. Acta.* 514:294–309.

Kimura, Y., K. Kurzydlowski, M. Tada, and D. H. MacLennan. 1996. Phospholamban regulates the Ca^{2+}-ATPase through intramembrane interactions. *J. Biol. Chem.* 271:21726–21731

Kimura, Y., K. Kurzydlowski, M. Tada, and D. H. MacLennan. 1997. Phospholamban inhibitory function is activated by depolymerization. *J. Biol. Chem.* 272:15061–15064.

Kranias, E. G. 1985. Regulation of Ca^{2+} transport by cyclic 3′,5′-AMP-dependent and calcium-calmodulin-dependent phosphorylation of cardiac sarcoplasmic reticulum. *Biochem. Biophys. Acta.* 844:193–199.

Kranias, E. G., F. Mandel, T. Wang, and A. Schwartz. 1980. Mechanism of the stimulation of calcium ion dependent adenosine triphosphatase of cardiac sarcoplasmic reticulum by adenosine 3′,5′-dependent protein kinase. *Biochemistry.* 19:5434–5439.

Lanzetta, P. A., L. J. Alvarez, P. S. Reinach, and D. A. Candia. 1979. An improved assay for nanomole amounts of inorganic phosphate. *Anal. Biochem.* 100:95–97.

Lowry, O., N. Rosebrough, A. Farr, and R. Randall. 1951. Protein measurement with the Folin phenol reagent. *J. Biol. Chem.* 193:265–275.

MacLennan, D. H., T. Toyofuku, and J. Lytton. 1992. Structure-function relationships in sarcoplasmic or endoplasmic reticulum type Ca^{2+} pumps. *Ann. N.Y. Acad. Sci.* 671:1–10.

Mahaney, J. E., J. P. Froehlich, and D. D. Thomas. 1995. Conformational transitions of the sarcoplasmic reticulum Ca-ATPase studied by time-resolved EPR and quenched-flow kinetics. *Biochemistry.* 34: 4864–4879.

McKenna, E., J. S. Smith, K. E. Coll, E. K. Mazack, E. J. Mayer, J. Antanavage, R. T. Wiedmann, and R. G. Johnson, Jr. 1996. Dissociation of phospholamban regulation of cardiac sarcoplasmic reticulum Ca^{2+} ATPase by quercetin. *J. Biol. Chem.* 271:24517–24525.

Movsesian, M. A., M. Karimi, K. Green, and L. R. Jones. 1994. Ca^{2+} transporting ATPase, phospholamban, and calsequestrin levels in nonfailing and failing human myocardium. *Circulation.* 90:653–657.

Negash, S., L. T. Chen, D. J. Bigelow, and T. C. Squier. 1996. Phosphorylation of phospholamban by cAMP-dependent protein kinase enhances interactions between Ca-ATPase polypeptide chains in cardiac sarcoplasmic reticulum membranes. *Biochemistry.* 35:11247–11259.

Porzio, M. A., and A. M. Pearson. 1977. Improved resolution of myofibrillar proteins with sodium dodecyl sulfate-polyacrylamide gel electrophoresis. *Biochim. Biophys. Acta.* 490:27–34.

Reddy, L. G., L. R. Jones, R. C. Pace, and D. L. Stokes. 1996. Purified, reconstituted cardiac Ca^{2+}-ATPase is regulated by phospholamban but not by direct phosphorylation with Ca^{2+}/calmodulin-dependent protein kinase. *J. Biol. Chem.* 271:14964–14970.

Sham, J. S. K., L. R. Jones, and M. Morad. 1991. Phospholamban mediates the β-adrenergic-enhanced Ca^{2+} uptake in mammalian ventricular myocytes. *Am. J. Physiol.* 261:H1344–H1349.

Shigekawa, M., J.-A. Finegan, and A. M. Katz. 1976. Calcium transport ATPase of canine cardiac sarcoplasmic reticulum. *J. Biol. Chem.* 251: 6894–6900.

Simmerman, H. K. B., and L. R. Jones. 1998. Phospholamban: protein structure, mechanism of action, and role in cardiac function. *Physiol. Rev.* 78:921–947.

Simmerman, H. K. B., Y. M. Kobayashi, J. M. Autry, and L. R. Jones. 1996. A leucine zipper stabilizes the pentameric membrane domain of phospholamban and forms a coiled-coil pore structure. *J. Biol. Chem.* 271:5941–5946.

Smith, P. D., G. W. Liesegang, R. L. Berger, G. Czerlinski, and R. J. Podolsky. 1984. A stopped-flow investigation of calcium ion binding by ethylene glycol bis(beta-aminoethyl ether)-*N, N′*-tetraacetic acid. *Anal. Biochem.* 143:188–195.

Sumida, M., T. Wang, F. Mandel, J. P. Froehlich, and A. Schwartz. 1978. Transient kinetics of Ca^{2+} transport of sarcoplasmic reticulum. *J. Biol. Chem.* 253:8772–8777.

Sumida, M., T. Wang, A. Schwartz, C. Younkin, and J. P. Froehlich. 1980. The Ca^{2+}-ATPase partial reactions in cardiac and skeletal sarcoplasmic reticulum. *J. Biol. Chem.* 255:1497–1503.

Tada, M., F. Ohmori, M. Yamada, and H. Abe. 1979. Mechanism of the stimulation of Ca^{2+}-dependent ATPase of cardiac sarcoplasmic reticulum by adenosine 3′:5′-monophosphate-dependent protein kinase. *J. Biol. Chem.* 254:319–326.

Tada, M., M. Yamada, F. Ohmori, T. Kuzuya, M. Inui. and H. Abe. 1980. Transient state kinetic studies of Ca^{2+}-dependent ATPase and calcium transport by cardiac sarcoplasmic reticulum. *J. Biol. Chem.* 255: 1985–1992.

Toyofuku, T., K. Kurzydlowski, M. Tada, and D. H. MacLennan. 1994a. Amino acids Glu^2 to Ile^{18} in the cytoplasmic domain of phospholamban are essential for functional association with the Ca^{2+}-ATPase of sarcoplasmic reticulum. *J. Biol. Chem.* 269:3088–3094.

Toyofuku, T., K. Kurzydlowski, M. Tada, and D. H. MacLennan. 1994b. Amino acids Lys-Asp-Asp-Lys-Pro-Val^{402} in the Ca^{2+}-ATPase of cardiac sarcoplasmic reticulum are critical for functional association with phospholamban. *J. Biol. Chem.* 269:22929–22932.

Voss, J. C., L. R. Jones, and D. D. Thomas. 1994. Physical mechanism of calcium pump regulation in the heart. *Biophys. J.* 67:190–196.